NASA Technical Memorandum 102692

AERODYNAMIC PARAMETERS OF HIGH-ANGLE-OF-ATTACK RESEARCH VEHICLE (HARV) ESTIMATED FROM FLIGHT DATA

VLADISLAV KLEIN

THOMAS P. RATVASKY

BRENT R. COBLEIGH

AUGUST 1990

National Aeronautics and Space Administration

Langley Research Center
Hampton, Virginia 23665

SUMMARY

Aerodynamic parameters of the High-Angle-of-Attack Research Aircraft (HARV) were estimated from flight data at different values of the angle of attack between 10° and 50°. The main part of the data was obtained from small amplitude longitudinal and lateral maneuvers. A small number of large amplitude maneuvers was also used in the estimation. The measured data were first checked for their compatibility. It was found that the accuracy of air data was degraded by unexplained bias errors. Then, the data were analyzed by a stepwise regression method for obtaining a structure of aerodynamic model equations and least squares parameter estimates. Because of high data collinearity in several maneuvers, some of the longitudinal and all lateral maneuvers were reanalyzed by using two biased estimation techniques, the principal components regression and mixed estimation. The estimated parameters in the form of stability and control derivatives, and aerodynamic coefficients were plotted against the angle of attack and compared with the wind tunnel measurements. The influential parameters are, in general, estimated with acceptable accuracy and most of them are in agreement with wind tunnel results. The simulated responses of the aircraft showed good prediction capabilities of the resulting model.

SYMBOLS AND ABBREVIATIONS

a_x, a_y, a_z	longitudinal, lateral, and vertical acceleration, g units
b	wing span, m
b_z	constant bias error in variable z
C_a	general aerodynamic force and moment coefficient
C_L	lift coefficient
C_ℓ, C_m, C_n	rolling-, pitching-, and yawing-moment coefficient
C_Y, C_Z	lateral- and vertical-force coefficient
$\bar{c}$	wing mean aerodynamic chord, m
d	a priori information
$E(\cdot)$	expected value
e	measurement-noise vector
g	acceleration due to gravity, m/sec^2
I_X, I_Y, I_Z	moments of inertia about longitudinal, lateral and vertical body axes, $kg\text{-}m^2$
I_{XZ}	product of inertia, $kg\text{-}m^2$
ℓ	number of regressor in adequate model
m	mass, kg
N	number of data points
n	number of regressors in regression equation
n_r	number of eigenvalues removed
P	matrix of known constants
p,q,r	roll rate, pitch rate, and yaw rate, rad/sec or deg/sec
$\bar{q}$	dynamic pressure, $\rho V^2/2$, Pa
R	measurement-noise covariance matrix
R^2	squared multiple correlation coefficient

r_n	rank of the X^TX matrix
S	wing area, m^2
$s(\cdot)$	standard error
s^2	variance estimate
T	thrust, N
t	time, sec
t*	t-statistic
t_j	eigenvector corresponding to λ_j
u,v,w	longitudinal, lateral, and vertical airspeed component, m/sec
V	airspeed, m/sec
W	covariance matrix of a priori information
X	matrix of regressors
Y	vector of dependent variables
y	dependent variable
z	vector of output variables
α	angle of attack, rad or deg
β	sideslip angle, rad or deg
δ_A	input variable expressing combined effect of aileron and differential tail and trailing edge flaps, rad or deg
δ_a, δ_r	aileron and rudder deflection, rad or deg
δ_{dh}	differential tail deflection, rad or deg
$\delta_h, \delta_f, \delta_{\ell f}$	horizontal tail and trailing and leading edge flap deflection respectively, rad or deg
ζ	random vector
η	vector of input variables
Θ	vector of unknown parameters

Θ_0, Θ_j	unknown parameters
θ, ϕ, ψ	pitch, roll, and yaw angle, rad or deg
λ_z	scale factor error of variable z
λ_j	j-th eigenvalue of $X^T X$ matrix
ν	vector of residuals
ρ	air density, kg/m^3
$\rho(\ )$	correlation coefficient

Abbreviations:

c.g.	center of gravity
m.a.c.	mean aerodynamic chord

Subscript:

E	measured value
ME	mixed estimator
PC	principal components estimator
$\circ$	initial value

Superscript:

$\hat{}$	unbiased estimated value
$\sim$	biased estimated value

Matrix exponent:

T	transpose matrix
-1	inverse matrix

Derivatives of aerodynamic coefficients C_a (a = Y, Z, ℓ, m, n) referenced to a system of body axes and derivatives of C_L referenced to a system of wind axes with the origin at the airplane center of gravity:

$$C_{a_p} = \frac{\partial C_a}{\partial \frac{pb}{2V}} \qquad C_{a_q} = \frac{\partial C_a}{\partial \frac{\bar{q}c}{2V}} \qquad C_{a_r} = \frac{\partial C_a}{\partial \frac{rb}{2V}}$$

$$C_{a_\alpha} = \frac{\partial C_a}{\partial \alpha} \qquad C_{a_\beta} = \frac{\partial C_a}{\partial \beta}$$

$$C_{a_{\delta j}} = \frac{\partial C_a}{\partial \delta_j}, \qquad j = A, a, dh, f, h, \ell f, r$$

INTRODUCTION

NASA began the High Alpha Technology Program (HATP) in 1988 with the main goal to accelerate the development of technologies which would expand high-angle-of-attack capabilities of future fighter aircraft. The flight research portion of the program has been using the High Angle-of-Attack Research Vehicle (HARV) which is a modified F/A-18 aircraft. One of the objectives of the flight program is to obtain low-speed, high-angle-of-attack aerodynamic parameters. These parameters may be used for validation of theoretical and wind tunnel predictions and for the development of a mathematical model of aircraft aerodynamics.

As reported in references 1 and 2, the first attempts to obtain accurate parameter estimates of the HARV from flight data were not very successful. The main reason was the insufficient excitation of response variables in maneuvers intended for parameter estimation. Low excitation of these variables was caused by poor selection of input forms and, in some cases, by difficulties in maneuvering the aircraft in the requested way. The accuracy of estimated parameters was further degraded by close relationships between deflections of various control surfaces introduced by the HARV control system, uncertainty in the model structure at high angles of attack, and inaccuracy of measured air data.

To avoid some of these problems, a new set of inputs was selected and verified in the flight simulator. Increased attention was given to the accuracy of measured incidence angles and to the extensive use of system identification methodology.

The purpose of this report is to present a quick release of parameter estimates from various sets of data, compare those estimates with the existing aerodynamic model in the flight simulator, and demonstrate the prediction capabilities of the model determined from flight data. The report starts with the description of the aircraft, and flight and wind tunnel data available. Then, procedures for data analysis are briefly outlined. The results that follow include checks on the compatibility of measured responses, variation of estimated parameters with the angle of attack, and comparison of these estimates with wind tunnel measurements. The existing inconsistencies in flight results and discrepancies between them and wind tunnel data are discussed. Finally, measured and predicted aircraft motion in small amplitude maneuvers are compared.

AIRCRAFT

The test vehicle is a twin-engine, single-seat fighter aircraft. It has a moderately swept wing with highly swept leading-edge extensions. The all-moving horizontal tail surfaces are mounted behind and below the wing; twin vertical tails are canted and toed out. The aircraft is controlled by four digital computers working in parallel. The computers are used in conjunction with redundant electrohydraulic servoactuators and analog sensors to provide primary control capabilities. There is also a backup mechanical control of the stabilator surfaces and open-loop analog control of the aileron and rudder. Longitudinal control uses symmetric deflections of the stabilator, leading edge and trailing edge flaps. Lateral control is provided by the ailerons, differential deflections of the stabilator, leading and trailing edge flaps, and synchronous rudder deflection. A drawing of the aircraft is presented in figure 1. The basic geometric, mass, and inertia characteristics are summarized in table I. A more detailed description of the aircraft and its control system is contained in references 3 and 4.

The test aircraft was modified by adding right- and left-wing-tip booms with Pitot-static heads and α- and β-vanes as shown in figure 1. Furthermore, flush pressure orifices were mounted on the forward radome area of the aircraft and on the remaining part of the forebody and leading-edge extension. The air data could be obtained from pressure measurements on the radome. The aircraft has a pulse-code modulation instrumentation system with telemetry as the only source of data. The measured data are recorded at the telemetry ground station. The instrumentation system includes transducers for the measurement of closed- and open-loop input variables, response variables, control system and engine operation, and fuel consumption from which instantaneous mass and inertia characteristics were calculated.

FLIGHT AND WIND TUNNEL DATA

The flight data of the tested aircraft were obtained from NASA Dryden Flight Research Facility in the form of time histories sampled at 50 samples/sec. The measured data were corrected for the c.g. offset of the linear accelerometers and wind vanes, and for the upwash and sidewash effects of the α- and β-vanes. The air data for the analysis were taken as the average values from the right- and left-boom sensors. Various maneuvers were initiated from mostly steady flights at altitudes between 5,000m and 12,000m (17,000 ft and 39,000 ft). In all maneuvers the Mach number did not exceed the value of 0.4. The scheduling of leading and trailing edge flaps with the angle of attack is shown in figure 2.

Three different sets of maneuvers were available for the analysis. The first set consisted of 32 longitudinal and 32 lateral small amplitude maneuvers at angles of attack between 10° and 50°. The pilot input for the longitudinal maneuvers was a pitch command usually applied as three doublets of various duration. For the lateral responses, separate yaw and roll commands in the form of simple doublets were used. Time histories of open-loop input and response variables from the maneuvers are presented in figures 3 and 4. In figure 3 both the longitudinal and lateral maneuvers at $\alpha \approx 13^\circ$ are shown. The inputs for the longitudinal maneuver included deflections of the horizontal tail, leading edge flaps, and trailing edge flaps. In the lateral maneuvers the input variables were the aileron, rudder, and differential tail deflections. Because of low airspeed (below 120m/sec) the control system did not move the differential leading and trailing edge flaps. Both maneuvers represent good excitation of all response variables. As expected, the control system introduced strong coupling between deflections of aileron and differential tail, and coupling between symmetric leading and trailing edge flaps deflection, and angle of attack. Figure 4 shows an example of similar maneuvers at $\alpha \approx 44^\circ$. From the time histories, problems of insufficient excitation of linear accelerations and maintaining uncoupled responses were visible. Because of the high values of α in these maneuvers the leading and trailing edge flaps remained in fixed position. On the other hand, strong coupling introduced by the control system existed between the aileron, differential tail, and rudder.

The second set of data included 14 large amplitude maneuvers; 4 longitudinal and 10 lateral. In each of these maneuvers, the motion was excited within the extended range of angle of attack, usually from 10° to 50°, using commanded doublets of various amplitudes and durations combined with a gradual increase of the horizontal tail deflection. One of the large amplitude lateral maneuvers is shown in figure 5. Finally, the last data set contained three quasi-steady deceleration-acceleration maneuvers.

The wind tunnel data of the F/A-18 aircraft are summarized in reference 3. The stability and control derivatives denoted as "wind tunnel" in this report were computed from aerodynamic functions used in the NASA Langley Research Center flight simulator of HARV under the following conditions: the Mach number of 0.4, altitude of 20,000 ft, c.g. location at

25 percent of the m.a.c., scheduled flaps position and horizontal tail deflection required to trim the aircraft at given angle of attack. The angles of attack varied between 2° to 54° with the increments of 2°. The aerodynamic coefficients C_L, C_D and C_m were obtained as functions of α for the above mentioned conditions but referred to $\delta = -6^\circ$.

FLIGHT DATA ANALYSIS

The first step in the analysis included a check on measured data compatibility and estimation of unknown bias errors in the measurements. Then, a structure of aerodynamic model equations was determined and unknown parameters, mostly in terms of stability and control derivatives, estimated. The accuracy of least squares estimates can be, however, degraded by near-linear dependency (collinearity) among measured time histories. The existence of data collinearity and its possible effect on the estimates were, therefore, estimated. As the result of that, some maneuvers had to be analyzed again using different estimation techniques which can reduce damaging effect of collinearity.

For the compatibility check the maximum likelihood method of reference 6 was applied. The state equations were represented by kinematic equations

$$\dot{x} = f(x, \eta, \Theta) \tag{1}$$

where

$$x = [u, v, w, \phi, \theta, \psi]^T$$

$$\eta = [a_x, a_y, a_z, p, q, r]^T$$

and Θ is a vector of unknown bias and scale factor errors in measured input and response variables. The vector of response variables was formulated as

$$z = [V, \beta, \alpha, \phi, \theta, \psi]^T$$

and each measured response variable was expressed as

$$z_E = (1 + \lambda_z)\, z + b_z + e_z \tag{2}$$

where λ_z is the unknown scale factor error, b_z is the constant bias error and e_z is the measurement noise. For the measured inputs η it was assumed that the scale factor errors and the measurement noise are equal to zero.

The unknown parameters and their Cramer-Rao bounds were obtained by minimizing

$$J = -\frac{1}{2}\sum_{i=1}^{N} \nu^T(i)\, R^{-1}\nu(i) - \frac{N}{2}\, n|R| \tag{3}$$

where

$$\nu(i) = z_E(i) - \hat{z}(i,\Theta)$$

R is the covariance matrix of measurement noise and N is the number of data points.

A stepwise regression of reference 7 was used for model structure determination and parameter estimation. In linear regression the aerodynamic model equations are formulated as

$$y = \Theta_0 + \Theta_1 x_1 + \ldots \Theta_n x_n \tag{4}$$

where y is the aerodynamic coefficient (dependent variable), x_1 to x_n are the measured response and input variables or their combinations (regressors) and Θ_j, $j = 0, 1, \ldots, n$ are the unknown parameters. The aerodynamic coefficients were calculated from the following expressions

$$C_L = \frac{mg}{\bar{q}S}(a_x \sin\alpha - a_z \cos\alpha) - \frac{T}{\bar{q}S}\sin\alpha$$

$$C_Y = \frac{mg}{\bar{q}S}\, a_y$$

$$C_Z = \frac{mg}{\bar{q}S}\, a_z \tag{5}$$

$$C_\ell = \frac{I_X}{\bar{q}Sb}\left[\dot{p} - \left(\frac{I_Y - I_Z}{I_X}\right)qr - \frac{I_{XZ}}{I_X}(pq + \dot{r})\right]$$

$$C_m = \frac{I_Y}{\bar{q}S\bar{c}}\left[\dot{q} - \left(\frac{I_Z - I_X}{I_Y}\right)pr - \frac{I_{XZ}}{I_Y}(r^2 + p^2)\right]$$

$$C_n = \frac{I_Z}{\bar{q}Sb}\left[\dot{r} - \left(\frac{I_X - I_Y}{I_Z}\right)pq - \frac{I_{XZ}}{I_Z}(\dot{p} - qr)\right]$$

In these equations the thrust was computed from the engine subroutine in the F/A-18 simulator for given M, h, and power lever angle. The angular accelerations were obtained by fitting cubic splines to measured angular velocities and subsequent differentiation of fitted curves.

Candidate regressors for the small amplitude maneuvers were postulated as

$$\alpha,\ q\bar{c}/2V,\ \delta_h,\ \delta_f,\ \delta_{\ell f},\ \alpha^2,\ \alpha^3,\ \alpha q\bar{c}/2V$$

$$\alpha\delta_h,\ \beta^2,\ V/V_0,\ |rb/2V|,\ |pb/2V|$$

and for the small amplitude lateral maneuvers as

$$\beta,\ pb/2V,\ rb/2V,\ \delta_a,\ \delta_r,\ \beta^2,\ \beta^3$$

$$\alpha\beta,\ \alpha pb/2V,\ \alpha rb/2V,\ \alpha\delta_a,\ \alpha\delta_r$$

$$\alpha^2\beta,\ \alpha^2 pb/2V,\ \alpha^2 rb/2V,\ \alpha^2\delta_a,\ \alpha^2\delta_r,\ \alpha$$

Because of linear relationship between δ_a and δ_{dh}, the differential tail deflection was combined with aileron deflection to introduce the following control effectiveness term

$$C_{a_{\delta A}} = C_{a_{\delta a}} + \frac{\delta_{dh}}{\delta_a} C_{a_{\delta dh}},\ a = Y,\ \ell,\ \text{or}\ n \qquad (6)$$

where δ_{dh}/δ_a was estimated from measured data as 0.420 ± 0.0066.

The large amplitude maneuvers were analyzed after partitioning an ensemble of data from repeated measurements into subsets of selected α-intervals, as described in reference 8. The distribution of data points in these subsets for longitudinal and lateral maneuvers is shown in figure 6. The regressors for the longitudinal and lateral subsets were postulated as

$$q\bar{c}/2V,\ \delta_h,\ \delta_f,\ \delta_{\ell f},\ \beta^2,\ \delta_h^2,\ \delta_h^3$$

and

$$\beta,\ pb/2V,\ rb/2V,\ \delta_a,\ \delta_r,\ \beta^3,\ \beta\delta_h,\ (pb/2V)^2,\ (pb/2V)^3$$

respectively.

Finally, for a single large amplitude longitudinal maneuver a model was formulated as

$$C_a = C_a(\alpha)_{\delta_h = -6^\circ} + C_{a_q}(\alpha)\,\frac{\bar{qc}}{2V} + C_{a_{\delta h}}(\alpha)\,\Delta\delta_h + C_{a_{\beta^2}}\,\beta^2 \qquad (7)$$

where

$$\Delta\delta_h = \delta_h - \frac{-6}{57.3} = \delta_h + 0.1047$$

The first three terms on the right hand side of eq. (7) were approximated by the first-order polynomial splines (see reference 9). The control terms $\Delta\delta_f$ and $\Delta\delta_{\ell f}$ were not included because of their small effect on the estimates of remaining parameters.

The unknown parameters in eq. (4) were obtained by minimizing the cost function

$$J = \sum_{i=1}^{N} \left[y(i) - \Theta_0 - \sum_{j=1}^{\ell} x_j(i)\,\Theta_j \right]^2 \qquad (8)$$

where ℓ is the number of statistically significant terms in eq. (4). The least squares estimates of unknown parameters were obtained as

$$\hat{\Theta} = (X^T X)^{-1} X^T Y \qquad (9)$$

where X is the matrix of regressors and ones, and Y is the vector of measured dependent variables. The covariance matrix of parameters was estimated as

$$\mathrm{Cov}\,(\Theta) = s^2 (X^T X)^{-1} \qquad (10)$$

where s^2 is the variance of the measurement noise. The square root of the variance can be interpreted as a fit error for aerodynamic coefficients. Its estimate is based on the residuals and has the form

$$s = \sqrt{\frac{\sum_{i=1}^{N} [y_E(i) - \hat{y}(i)]^2}{N - \ell}} \qquad (10)$$

In some cases t-statistics (the t-distribution) should be included if the interest is focused on the significance of parameters. The estimates of these statistics are given as

$$t_j^* = \frac{\Theta_j}{s(\Theta_j)} \qquad (11)$$

The possibility of data collinearity in measured data was investigated by procedures described in reference 10. They include

a) Examination of the correlation matrix X^TX where the regressors are standardized (centered and scaled to unit length).

b) Eigensystem analysis of the X^TX matrix. The eigenvalues close to zero indicate near-linear dependency in the data. As a measure of the spread of the eigenvalues of X^TX, the condition number, defined as the ratio of the maximum to minimum eigenvalue, is used. Condition numbers between 100 to 1000 imply moderate to strong collinearity.

c) Parameter variance decomposition into a sum of components, each corresponding to one, and only one, of the eigenvalues of X^TX. An unusually high proportion in the variance of two or more parameters for the same small eigenvalue can provide evidence that the near dependency is causing problems.

The application of the ordinary least-squares technique to a set of collinear data very often results in nonphysical values for parameters and large values of their covariance. In order to obtain more stable and accurate estimates, two biased estimation techniques of reference 10, the principal components regression and mixed estimation, were applied to maneuvers where data collinearity was detected. These techniques provide estimates which are biased but have smaller variance than that of the least squares estimates.

The principal components regression technique uses orthogonal regressors rather than the original ones. The orthogonal regressors are arranged in order of decreasing eigenvalues of X^TX. Then, the last n_r of these eigenvalues are removed from the analysis and the least squares principle is applied to the remaining components. Then, the parameter estimates associated with the orthogonal regressors are transformed back to the set of original parameters. The principal components estimator of Θ thus takes the form

$$\tilde{\Theta}_{PC} = \sum_{j=1}^{n+1-n_r} \frac{1}{\lambda_j} t_j^T X^T Y t_j \tag{12}$$

and the covariance matrix has the form

$$\mathrm{cov}(\Theta_{PC}) = s^2 \sum_{j=1}^{n+1-n_r} \frac{1}{\lambda_j} t_j t_j^T \tag{13}$$

where λ_j are the eigenvalues of the X^TX and t_j is the eigenvector corresponding to λ.

The assumption of an integral rank for X can sometimes be too restrictive, especially if the number of regressors is small. A possible improvement to the principal components estimator, known as the fractional rank estimator, has been proposed in reference 11.

The mixed estimation is a procedure which uses prior information

$$d = P\Theta + \zeta \tag{14}$$

to augment the measured data. The mixed estimator is obtained as

$$\tilde{\Theta}_{ME} = \left[\frac{1}{s^2} X^TX + P^TW^{-1}P\right]^{-1} \left[\frac{1}{s^2} X^TY + P^TW^{-1}d\right] \tag{15}$$

with covariance matrix

$$\text{cov}(\Theta_{ME}) = \left[\frac{1}{s^2} X^TX + P^TW^{-1}P\right]^{-1} \tag{16}$$

In eq.(14) to eq. (16) ζ is a vector of random variables with $E(\zeta) = 0$ and $E(\zeta\zeta^T) = W$, and P is a matrix of known constants.

RESULTS AND DISCUSSION

The results of the flight data analysis are summarized in the following six sections. The first one describes the estimates of bias errors in measured data and the compatibility between measured and predicted time histories of response variables. In the second section, structures of adequate models for longitudinal and lateral maneuvers are presented. This section is followed by investigation of data collinearity and by measures taken to avoid its damaging effect on parameter estimates. The next two sections include estimated longitudinal and lateral parameters and their comparison with wind tunnel data. The last section presents three examples demonstrating prediction capabilities of the resulting model.

Data Compatibility Check:

A selected number of longitudinal and all lateral maneuvers were analyzed to obtain estimates of bias errors in the measured response variables, and residuals represented by differences between measured and predicted response variables. The parameter estimates indicated a need for additional corrections to the measured data, and the residuals provided information about bounds on the remaining errors in the measured data. The results from the longitudinal and lateral maneuvers in figure 3 are presented as an example. The parameter estimates and their standard errors are given in tables II and III; the time histories of output variables and corresponding residuals in figures 7 and 8. The estimates indicate small errors in angular rates, Euler angles and angle of attack, larger errors in longitudinal and lateral accelerations, and an excessive scale factor error in the sideslip angle. Similar conclusions could be drawn from the remaining maneuvers. Because the analysis of small amplitude maneuvers uses the increments of measured variables, the main concern was the large scale factor error in sideslip angle. The estimates of λ_β from various maneuvers varied randomly with no apparent dependence on the angle of attack or magnitude of sideslip angle. The average value of λ_β obtained from 32 small amplitude maneuvers was equal to 0.130 with an ensemble standard error of 0.097. Each sideslip angle time history was corrected by using the estimates of λ_β corresponding to that maneuver. The estimates of the scale factor errors for α also varied randomly around zero not exceeding the value of 0.02. For that reason no corrections to the angle of attack were applied.

The residuals in figures 7 and 8 still include the effect of uncorrected bias errors. The magnitude of these errors is mainly visible in the air data variables. By examining all maneuvers it was found that the bias errors in measured air data have bounds equal to ±3 m/sec for the airspeed and ± 1° for both α and β. In some maneuvers for $\alpha > 40°$ the bounds for V and β were increased to ± 5 m/sec and ± 2.5°, respectively. The bias errors in the air data are usually related to one short segment of the whole maneuver. Despite this, the quoted inaccuracy in the air data measurement is unacceptable for a serious research test. The main factor contributing to these errors is the location of the vanes and Pitot-static

heads. Because this arrangement cannot be changed, it is necessary in future data compatibility checks to consider changes in the postulated model. Possible changes may be to include measured position of the aircraft and/or to include more unknown parameters in the measurement equation. The other possibility is to use the flush air data system after its performance is checked.

Adequate Models for Aerodynamic Coefficients:

A stepwise regression method was applied to each set of transient data. As a result, adequate models for the aerodynamic model equations were determined and the least squares estimates of parameters in the model obtained. The selection of these models was based mainly on changes in the multiple correlation coefficient, R^2, with an increasing number of terms included in the model. In addition to this criterion, the fit error and statistical significance of the estimates were examined and the residuals checked for unexplained differences between measured and predicted aerodynamic coefficients. More about the selection of an adequate model can be found in reference 7. An example of measured and predicted aerodynamic coefficient is given in figure 9. These coefficients correspond to the lateral maneuver shown in figure 3. In this example the residuals reflect the effect of rather excessive measurement noise and model inadequacy.

A general form of an adequate model for longitudinal small amplitude maneuvers was determined as

$$C_a = C_{a_{\delta h=-6^\circ}} + C_{a_\alpha}\Delta\alpha + C_{a_{\alpha^2}}\Delta\alpha^2 + C_{a_{\alpha^3}}\Delta\alpha^3$$

$$+ C_{a_{\beta^2}}\beta^2 + C_{a_q}\frac{q\bar{c}}{2V} + C_{a_{\delta h}}\Delta\delta_h + C_{a_{\delta f}}\Delta\delta_f \qquad (17)$$

$$+ C_{a_{\delta \ell f}}\Delta\delta_{\ell f}\,, \qquad a = L,\ Z,\ \text{or}\ m$$

The reference conditions in this model correspond to trimmed α, scheduled flaps position and $\delta_h = -6^\circ$. Therefore,

$$\Delta\alpha = \alpha - \alpha_0$$

$$\Delta\delta_f = \delta_f - \delta_{f_0}$$

$$\Delta\delta_{\ell f} = \delta_{\ell f} - \delta_{\ell f_0}$$

$$\Delta\delta_h = \delta_h + 0.1047$$

In many maneuvers, especially those with small excitation, a linear model was found to be the best. The leading and trailing edge flap derivatives appeared significant only in a limited number of maneuvers for α between 10° to 26°.

Adequate models for lateral small amplitude maneuvers have the form

$$C_a = C_{a_0} + C_{a_\beta}\beta + C_{a_{\beta^3}}\beta^3 + C_{a_p}\frac{pb}{2V} + C_{a_r}\frac{rb}{2V} + C_{a_{\delta_a}}\delta_a + C_{a_{\delta_r}}\delta_r, \qquad a = Y, \ell, \text{ or } n \tag{18}$$

The cubic term in β was significant only in models for the rolling-moment coefficient with α between 35° to 40°.

Models for partitioned data usually included linear terms only. Many stability and control derivatives could not be estimated because of low significance of associated regressors. For a single large amplitude longitudinal maneuver, first-order splines were adequate for the approximation of coefficients and derivatives. As in the case of partitioned data, low excitation of the short-period mode prevented more detailed determination of model structure.

Effect of Data Collinearity on Parameter Estimates:

After determining model structures and estimating parameters, several small amplitude maneuvers were checked for data collinearity and its possible effect on parameter estimates. Two examples of these checks are given. The first one uses data from the longitudinal maneuver in figure 3. An adequate model for the pitching-moment coefficient includes eight regressors. The X^TX matrix in correlation form and eigenvalues of the X^TX matrix are presented in table IV. Two high pairwise correlations (α, $\delta_{\ell f}$) and (α, α^3) exist. The condition number of 647 indicates a moderately strong effect of data collinearity on parameter estimates. For that reason the covariance decomposition proportions were not included in table IV. The least squares parameter estimates are summarized in table V. They are compared with the results of mixed estimation using $C_{m_{\delta\ell f}} = 0.083 \pm 0.013$ as a loose a priori value. Table V also includes the standard errors and t-statistics of parameters and fit errors, $s(C_m)$, for both techniques. From the comparison of results it follows that all parameters in the model, with the exception of the least squares estimates of $C_{m_{\delta\ell f}}$, are statistically significant ($t^* > 1.96$). The differences between the two sets of parameters are within 2σ-bounds, but the introduction of a priori information sharpens the regression results. Based on this observation the maneuvers with leading- and trailing-edge flaps active were analyzed again using the mixed estimation technique. The new parameter estimates represent the final results discussed in the next section.

In the second example, the data collinearity diagnostic for a lateral maneuver at $\alpha \approx 41^{\circ}$ is presented in table VI. In this maneuver strong correlation exists between the aileron and rudder deflection. The spread of eigenvalues is very small, however, resulting in a condition number equal to 47. The effect of strong pairwise correlation $\rho(\delta_a, \delta_r)$ on parameters in the rolling-moment equation is demonstrated in table VII by using three different estimation techniques. The results from consecutive parameter entries of the stepwise regression algorithm show the change in the value of $C_{\ell_{\delta A}}$ from -0.041 to -.102 when the regressor δ_r enters the model. This sudden change is a direct result of strong correlation between δ_a and δ_r. When the mixed estimation with an a priori value of $C_{\ell_{\delta r}} = 0.000 \pm 0.010$ was introduced, the value of $C_{\ell_{\delta A}} = 0.055$ was obtained. This value agrees well with the wind tunnel prediction of $C_{\ell_{\delta A}}$. The estimates of $C_{\ell_{\delta A}}$ were further verified by using the principal components regression. The reduction of rank of matrix $X^T X$ from 6 to 5 was too coarse, as shown by the resulting fit error. Therefore, several partial rank reductions were tried. For a rank of 5.5, both the fit error and parameters were almost identical to those from the mixed estimation. The t-statistics indicate that, in all cases, the parameters C_{ℓ_p} and C_{ℓ_r} have low significance in the model. In this example an adequate model would have only three regressors, β, δ_a, and δ_r, which is also indicated by the values of the squared multiple correlation coefficient.

Because of the damaging effect of the aileron-rudder correlation on parameter estimates, the collinearity diagnostic was performed on all lateral maneuvers. The resulting correlation coefficient, $\rho(\delta_a, \delta_r)$, is plotted against the angle of attack in figure 10. It can be expected that the least squares estimates of the control parameters from maneuvers at $\alpha > 20^{\circ}$ can be influenced by this correlation. All the lateral maneuvers were, therefore, analyzed again and the mixed estimates were selected as the final set of parameters. The a priori values of $C_{Y_{\delta A}}$, $C_{\ell_{\delta r}}$ and $C_{n_{\delta A}}$ were based on wind tunnel data. The uncertainty in these values was expressed by standard errors varying between 0.02 to 0.04. The level of uncertainty was kept as high as possible depending on the correlation between estimated control parameters. Values of this correlation coefficient less than 0.85 were considered acceptable.

Longitudinal Parameters:

The longitudinal parameters include three coefficients, C_L, C_Z and C_m, and their derivatives plotted against the angle of attack. The three coefficients corresponding to steady conditions with scheduled flaps and

fixed horizontal tail deflection, $\delta_h = -6^\circ$, are presented in figures 11 to 13. In figure 11 the wind tunnel measurement of C_L is compared with flight results from a slow deceleration/acceleration maneuver. The values from both parts of the maneuver agree quite well, but for α between 15° to 45° they are slightly lower than those from the wind tunnel measurement. The flight data of C_L and C_Z in figure 12 contain the results from small amplitude maneuvers and from a single large amplitude maneuver. The agreement between both sets is very good. The flight data of C_L are closer to the wind tunnel curve than the values of C_Z which have lower values almost over the whole range of α. Figure 13 presents the C_m coefficients estimated from small amplitude maneuvers, partitioned data and single large amplitude maneuvers. All three sets of flight results agree well. Some differences exist, however, between flight and wind tunnel measurement in the region of α between 20° and 40°.

The derivatives of longitudinal coefficients with respect to α are plotted in figure 14. They agree, in general, with the wind tunnel predictions. The only pronounced disagreement can be seen in the parameter C_{m_α} around $\alpha = 40^\circ$ where the flight data do not indicate a sudden increase of static stability as the wind tunnel test does. The q-derivatives are given in figure 15. Both the C_{L_q} and C_{Z_q} parameters are in sharp disagreement with the wind tunnel data for $\alpha < 40^\circ$. These differences have only a small effect on the prediction of aircraft motion because of the low significance of the corresponding terms in the model. Parameter values of C_{m_q} from small amplitude maneuvers and partitioned data indicate a sudden increase in damping at $\alpha \approx 22^\circ$ which was not predicted by wind tunnel measurement. Different values of C_{m_q} from the large amplitude maneuver for α between 12° to 22° might be the result of limited information in the data which prevented more refined determination of $C_{m_q}(\alpha)$ variation. For apparently the same reason no estimates of C_{m_q} for $\alpha > 38^\circ$ were obtained from partitioned data.

Figure 16 presents control derivatives related to horizontal tail deflection. All three parameters indicate lower tail effectiveness than that predicted from wind tunnel measurement. Large inconsistency exists in the $C_{m_{\delta h}}$ estimates from three different sets of data. The differences are sometimes greater than 0.1 which is greater than 15 percent of the estimated values. The large scatter in the estimates is surprising because the term $C_{m_{\delta h}} \Delta\delta_h$ is the most significant in the model which means that $C_{m_{\delta h}}$ should be

very well identifiable. At the same time the standard errors of the $C_{m_{\delta h}}$ estimates were low, varying between 0.005 to 0.014. No reasons for the low accuracy of $C_{m_{\delta h}}$ parameters were found.

The parameters expressing the effect of flaps are given in figures 17 and 18. The trailing-edge derivatives confirmed the trend in these parameters with the angle-of-attack change. The closeness of the leading-edge derivatives to the wind tunnel data is caused by their selection as a priori values in the mixed estimation and, at the same time, their low sensitivity.

Lateral Parameters:

The lateral stability and control parameters obtained from flight and wind tunnel measurements are included in figures 19 to 23. All the lateral parameters in a linear model were estimated from small amplitude maneuvers with different levels of consistency. The scatter in the estimates indirectly indicated the significance of corresponding terms in the model equations. Only the most important parameters were estimated from partitioned data, because the remaining parameters did not enter the model during the stepwise regression analysis.

The flight and wind tunnel sideslip derivatives are compared in figure 19. The differences in C_{Y_β} for α less than 35° and greater than 40°, and the differences in C_{ℓ_β} around $\alpha = 22^\circ$ could not be explained. The decrease in directional stability in flight for $\alpha > 40^\circ$ is caused by the horizontal tail setting. The wind tunnel data correspond to $\delta_h = 0^\circ$ whereas during the flight maneuvers at $\alpha > 40^\circ$ the tail deflection varied around $\delta_h = -11^\circ$.

Figure 20 contains the derivatives with respect to roll rate. The C_{Y_p} parameter varies substantially around the wind tunnel data with a tendency for large negative values for $\alpha > 40^\circ$. The parameter C_{ℓ_p} exhibits gradual decrease in the roll-damping with the increase of α. The difference between flight and wind tunnel results in the region of α between 25° to 42° could be the result of different types of maneuvers. Flight data were obtained from transient maneuvers while the wind tunnel testing was based on forced oscillations with small amplitude in roll angle equal to 5°. The variation of cross-derivative C_{n_p} for α less than 38° is similar to that from the wind tunnel test. For $\alpha > 40^\circ$, however, the flight data indicate an increase in negative values of this parameter.

The yaw-rate parameters are included in figure 21. Low excitation of yawing velocity in transient maneuvers and low contribution of yaw-rate terms to the lateral motion is reflected in large scatter of all three parameters. The resulting parameters are close to the wind tunnel prediction for $\alpha < 40^{\circ}$. For $\alpha > 40^{\circ}$ there is a change in C_{Y_r} to higher values and in C_{ℓ_r} from positive to negative value. All the control parameters in figures 22 and 23, except $C_{n_{\delta A}}$, were estimated with high consistency and closeness to the wind tunnel data. The values of the adverse-aileron-effect parameter, $C_{n_{\delta A}}$, are consistently lower than those from wind tunnel measurements.

Model Prediction Capabilities:

The prediction capabilities of the model determined from flight data were checked in several longitudinal and lateral maneuvers not used in the previous analysis. For each type of motion, the simulation was based on models with three degree-of-freedom. The remaining variables in the equations of motion were substituted by measured values.

One of the simulated longitudinal maneuvers at $\alpha \approx 32^{\circ}$ is presented in figure 24 where the time histories of the input variable and three output variables are plotted. The frequency of the motion is predicted very well. There are some discrepancies in the amplitudes of all three output variables. The remaining two figures include the predicted and measured lateral maneuvers. As in the previous case, the time histories of input and output variables are given. The first maneuver presented in figure 25 compares the measured and predicted output variables excited at $\alpha \approx 12^{\circ}$. The agreement between the two sets of data is very good. The second maneuver in figure 26 was performed at $\alpha \approx 48^{\circ}$. In this high-$\alpha$ maneuver the prediction differs from the measurement, but the main features of the response are predicted quite well. The deterioration of model prediction capabilities with increasing angle of attack was also observed in the remaining simulated maneuvers.

CONCLUDING REMARKS

Aerodynamic parameters of the High-Angle-of-Attack Research Vehicle (HARV) were estimated from different types of maneuvers at angles of attack varying between 10° and 50°. Data analysis included the data compatibility check, model structure determination, and parameter estimation. For these three steps a maximum likelihood estimation, stepwise regression, and three additional estimation techniques: the ordinary least squares, principal components regression, and mixed estimation, were applied. The resulting parameter estimates were obtained in the form of stability and control derivatives and aerodynamic coefficients. They were then presented as variations with the angle of attack and compared with wind tunnel measurements. In addition to the data analysis, the model prediction capability was checked. From all the results obtained the following conclusions can be drawn:

1. The data compatibility check showed good agreement between measured and predicted attitude angles. Some unexplained errors existed, however, in the air data. The error bounds for α and β were $\pm 1^\circ$ with an increase up to $\pm 2.5^\circ$ for β in some maneuvers with α above 40°. The effect of these errors on parameter estimation was not investigated.

2. Most of the adequate models for aircraft aerodynamic coefficients contained only linear terms with stability and control derivatives. For the longitudinal maneuvers with large excursions and lateral maneuvers for angles of attack between 25° and 42°, the adequate models also included nonlinear terms in α and β.

3. Increased data collinearity was present in longitudinal maneuvers with extensive excitation and leading edge and trailing edge flaps operating. In lateral maneuvers the near linear dependency existed among the aileron, differential tail, and rudder deflections. For the data with high collinearity, the mixed estimates of parameters were found more accurate than the estimates obtained by the ordinary least squares technique.

4. The lift, vertical-force, and pitching-moment coefficients estimated from different types of maneuvers as functions of angle of attack are in general agreement with wind tunnel tests.

5. From the measured data it was possible to estimate all stability and control derivatives. However, the accuracy of these estimates and their closeness to wind tunnel data vary substantially. Lateral control parameters are estimated with high consistency and are very close to the wind tunnel data. Larger scatter than expected existed in the estimates of the horizontal tail effectiveness. These parameters also have lower values than those predicted by wind tunnel measurement. All static stability parameters are estimated with acceptable accuracy expressed by their scatter. Unexplained departures from wind tunnel data exist in the longitudinal static stability parameter for angle of

attack around 40°, dihedral-effect parameter around $\alpha = 22°$, and in the lateral force parameter for almost the entire range of angle of attack. Almost all the dynamic parameters exhibit large scatter due to their low sensitivity. The most important differences between wind tunnel and flight data are in the damping-in-roll parameter and rolling-moment-due-to-yawing parameter. The flight results do not indicate an increase in roll damping between angles of attack of 25° and 42° as shown by wind tunnel data. Values of rolling moment with yawing velocity, C_{ℓ_r}, change from positive to negative for angles of attack greater than 40°.

The future experiment and data analysis should include the following:

1. Maneuver for the assessment of data compatibility and accuracy using air data from the wing-boom sensors and flush air data system.

2. Different types of maneuvers for obtaining parameters with increased accuracy.

3. Evaluation of measured data accuracy and different estimation techniques on the accuracy of parameter estimates.

4. More theoretical development in techniques for model structure determination and parameter estimation from flight data with high collinearity.

REFERENCES

1. Klein, Vladislav; Breneman, Kevin P.; and Ratvasky, Thomas P.: "Aerodynamic Parameters of an Advanced Fighter Aircraft Estimated From Flight Data. Preliminary Results," NASA TM-101631, 1989.

2. Breneman, Kevin P.: "Medium and High-Angle-of-Attack Aerodynamic Characteristics of an Advanced Fighter Aircraft Estimated From Flight Data," M.S. Thesis, The George Washington University, Washington, DC, 1989.

3. Anon: "F/A-18 Basic Aerodynamic Data," MDC A8575, McDonnell Aircraft Company, 1984.

4. Anon: "F/A-18 Flight Control Design Report," Vol. I and II, MDC A7813, McDonnell Aircraft Company, 1982.

5. Anon: "F/A-18 Stability and Control Data Report," Vol. I and II, MDC A7247, McDonnell Aircraft Company, 1982.

6. Klein, Vladislav; and Morgan, Dan R.: "Estimation of Bias Errors in Measured Airplane Responses Using Maximum Likelihood Methods," NASA TM-89059, 1987.

7. Klein, Vladislav; Batterson, James G.; and Murphy, Patrick C.: "Determination of Airplane Model Structure From Flight Data by Using Modified Stepwise Regression," NASA TP-1916, 1981.

8. Batterson, James G.; and Klein, Vladislav: "Partitioning of Flight Data For Aerodynamic Modeling of Aircraft at High Angle of Attack," Journal of Aircraft, Vol. 26, No. 4, April 1989, pp. 334-339.

9. Klein, Vladislav; and Batterson, James G.: "Determination of Airplane Model Structure From Flight Data Using Splines and Stepwise Regression," NASA TP-2126, 1983.

10. Klein, Vladislav: "Two Biased Estimation Techniques in Linear Regression. Application to Aircraft," NASA TM-100649, 1988.

11. Hocking, R. R.; Speed, F. M.; and Lynn, M. J.: "A Class of Biased Estimators in Linear Regression," Technometrics, Vol. 18, No. 4, November 1976, pp. 425-437.

Table I. Geometric, Mass and Inertia Characteristics of the Aircraft

Total Length, m	17.07
Wing:	
Area, m^2	37.16
Span, m	11.41
Mean geometric chord, m	3.51
Aspect ratio	3.5
Quarter-chord sweep angle, deg	20.0
Horizontal tail:	
Area (wetted), m^2	16.35
Span, m	6.58
Mean geometric chord, m	1.91
Aspect ratio	2.40
Quarter-chord sweep angle, deg	42.8
Moment arm (c.g. at 0.25 m.a.c.), m	5.12
Vertical tail:	
Area (wetted), m^2	9.66
Mean geometric chord, m	2.13
Aspect ratio	1.20
Quarter-chord sweep angle, deg	35.0
Cant, deg	20.0
Moment arm (c.g. at 0.25 m.a.c.), m	3.10
Mass, kg	14,400
Inertia:	
I_x , $kg\text{-}m^2$	28,880
I_y , $kg\text{-}m^2$	165,930
I_z , $kg\text{-}m^2$	185,030
I_{xz} , $kg\text{-}m^2$	-2,630

Table II. Estimates of Bias Errors in Measured Longitudinal Data

Parameter	$\hat{\theta}$	$s(\hat{\theta})$
b_V, m/sec	-.14	.035
λ_α	-.010	.0014
b_α, deg/sec	-.0106	.00020
b_θ, deg	-.386	.0039
λ_θ	.0505	00040
b_{ax}, g units	.152	.0021
b_{az}, g units	.061	.0023

Table III. Estimates of Bias Errors in Measured Lateral Data

Parameter	$\hat{\theta}$	$s(\hat{\theta})$
b_β	-0.54	0.023
λ_β	0.171	0.0029
b_p, deg/sec	-0.1564	0.00075
b_r, deg/sec	-0.0729	0.00071
b_ϕ, deg	-0.087	0.0094
λ_ϕ	0.071	0.0011
λ_φ	0.063	0.0013
b_{ay}, g units	-0.111	0.0027

Table IV. Collinearity Diagnostic for Longitudinal Maneuver

X^TX matrix (scaled and centered regressors):

α	$q\bar{c}/2V$	δ_h	δ_f	$\delta_{\ell f}$	α^2	α^3
1.000	.223	.016	.229	.775	-.313	.881
	1.000	.003	.193	-.206	-.079	.227
		1.000	-.487	.367	.575	-.042
			1.000	.007	-.687	.325
				1.000	-.579	.648
					1.000	-.470
						1.000

eigenvalues (scaled regressors):

3.190, 2.559, 1.125, .588, .301,

.156, .0765, .00493

Table V. Least Squares and Mixed Estimates, Longitudinal Maneuver

Parameter	Least squares estimation			Mixed estimation*		
	$\hat{\theta}$	$s(\hat{\theta})$	t*	$\hat{\theta}$	$s(\hat{\theta})$	t*
C_{m_o}	.079	.0016	50.6	.0852	.00096	84.9
C_{m_α}	- .09	.030	3.1	- .06	.017	3.2
$C_{m_{\alpha^2}}$	- 1.90	.075	25.4	- 1.88	.074	25.5
$C_{m_{\alpha^3}}$	-15.	1.0	14.9	-14.6	.99	14.8
C_{m_q}	- 4.3	.85	5.1	- 5.4	.49	11.1
$C_{m_{\delta h}}$	- .816	.0091	89.5	- .852	.0070	117.9
$C_{m_{\delta f}}$	.099	.0098	10.1	.107	.0081	13.2
$C_{m_{\delta \ell f}}$	- .04	.024	1.7	- .07	.013	5.6
$s(C_m)$	- .00565	-	-	.00565	-	-

*) a priori value $C_{m_{\delta \ell f}} = - .083 \pm .015$

Table VI. Collinearity Diagnostic for Lateral Maneuver

X^TX matrix (scaled and centered regressors)

β	pb/2V	rb/2V	δ_a	δ_r
1.000	- .083	- .014	- .009	.058
	1.000	.728	.053	- .177
		1.000	.111	.045
			1.000	.944
				1.000

eigenvalues (scaled regressors):

1.9888, 1.738, 1.172, .819, .239, .0426

Table VII. Least Squares and Biased Estimates, Lateral Maneuver

Parameter	Stepwise regression					Mixed estimation*	Principal components	
	n = 2	n = 3	n = 4	n = 5	n = 6		r_n = 5	r_n = 5.5
C_{ℓ_0}	-.0022	-.0005	-.0000	-.0000	-.0000	.0008	.0010	.0008
C_{ℓ_β}	-.103	-.102	-.106	-.106	-.106	-.103	-.102	-.103
	[36.3]	[42.9]	[47.1]	[47.3]	[47.3]	[45.2]	[44.7]	[44.8]
C_{ℓ_p}	-	-	-	-.05	-.03	-.05	-.09	-.05
				[3.0]	[1.8]	[2.1]	[3.9]	[1.9]
C_{ℓ_r}	-	-	-	-	-.05	-.07	-.05	-.08
					[1.5]	[1.5]	[1.0]	[1.6]
$C_{\ell_{\delta A}}$	-	-.041	-.102	-.095	-.095	-.055	-.019	-.059
		[17.0]	[44.2]	[41.2]	[41.2]	[12.7]	[14.0]	[12.8]
$C_{\ell_{\delta r}}$	-	-	.0145	.0126	.0128	.0033	.0046	.0047
			[27.9]	[24.4]	[28.8]	[8.8]	[17.2]	[4.6]
$s(C_\ell)$	.00500	.00418	.00396	.00394	.00394	.00408	.00429	.00413
R^2	66.0	76.2	78.7	78.9	79.0	-	-	-

*) a priori value $C_{\ell_{\delta r}} = .000 \pm .0010$

Note: figures in brackets are t - statistics

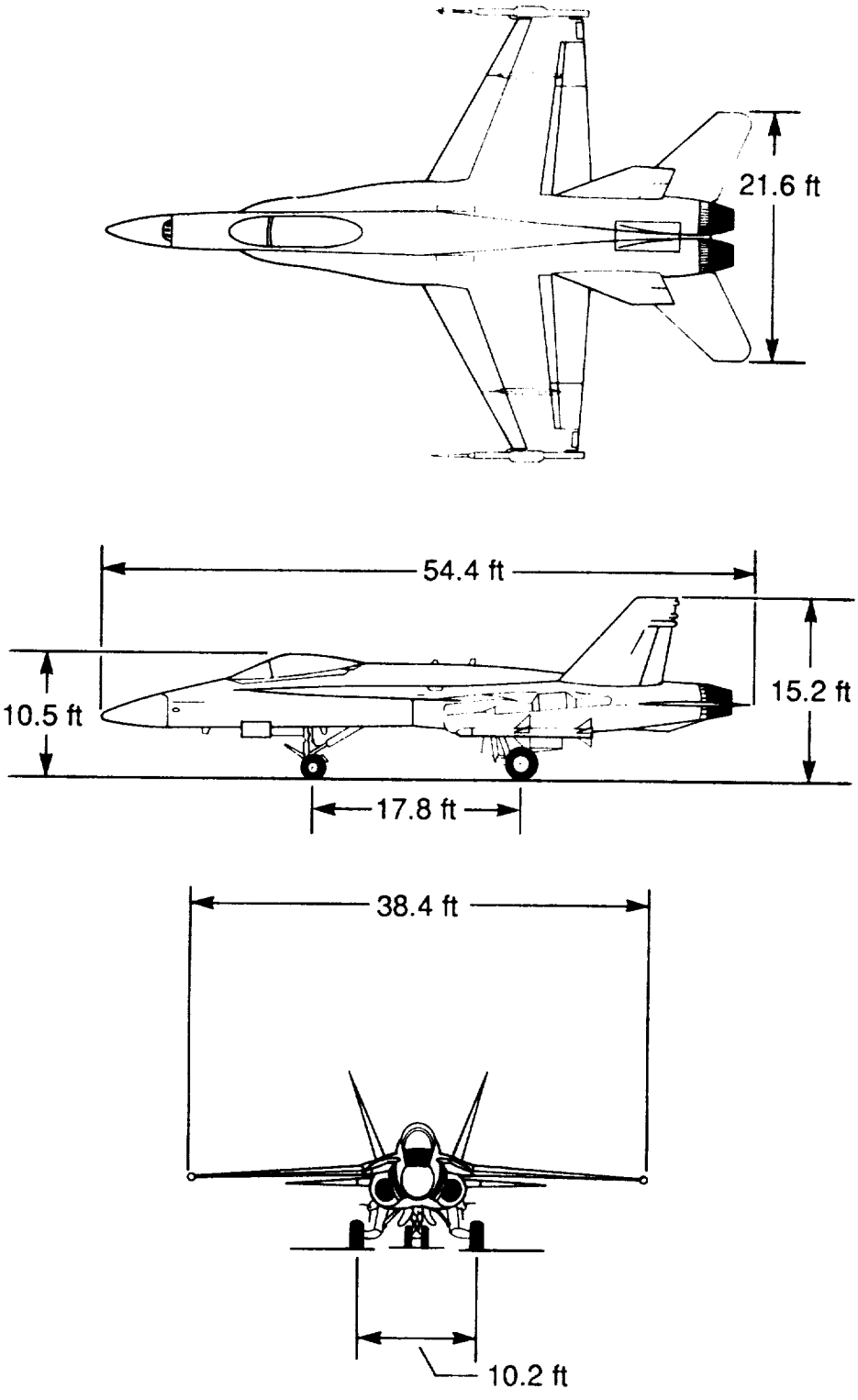

Figure 1. Three-view drawing of test aircraft.

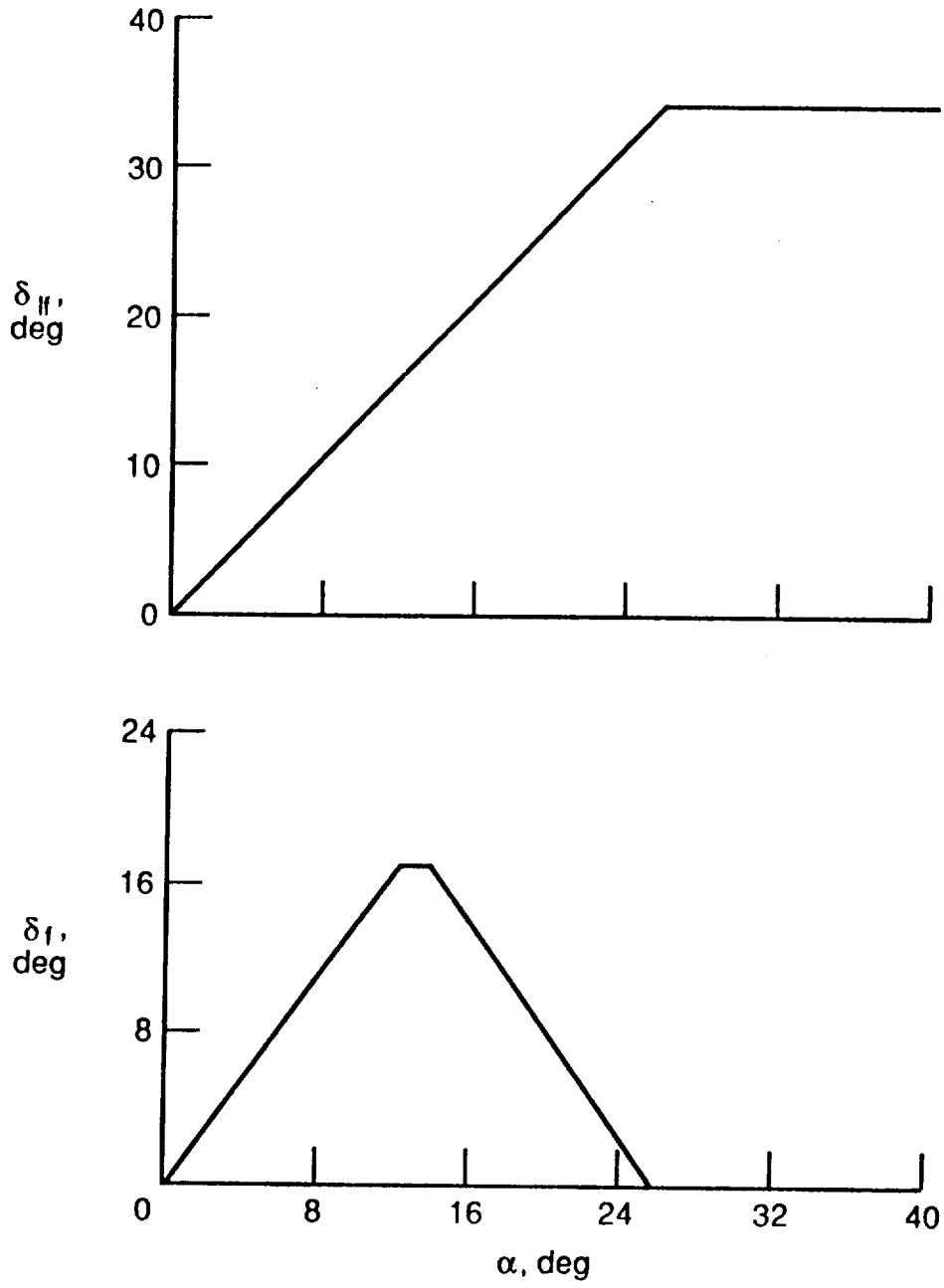

Figure 2. Leading and trailing edge flap schedule with angle of attack.

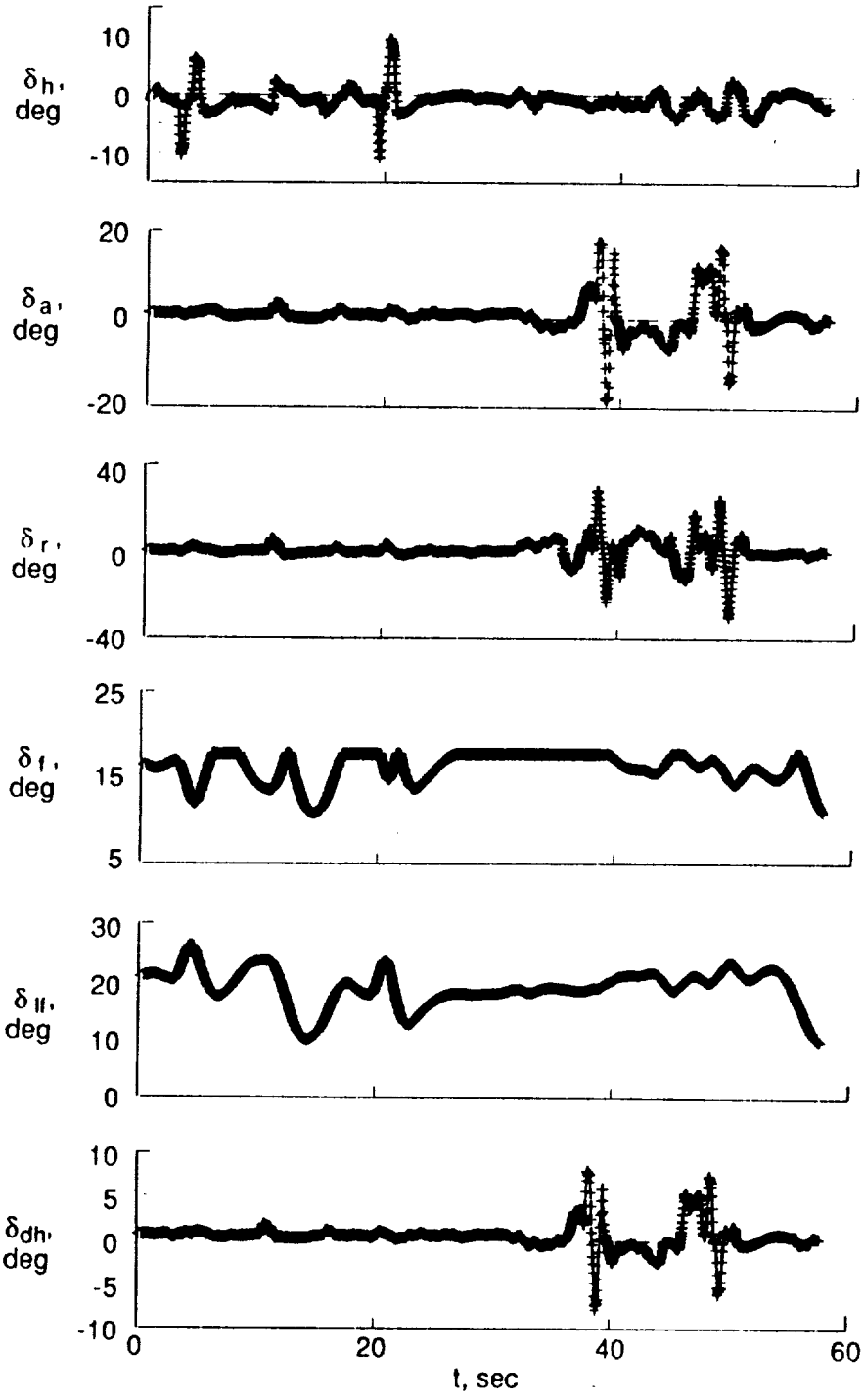

Figure 3. Time histories of measured input and response variables in small amplitude longitudinal and lateral maneuver ($\alpha \approx 13^{O}$).

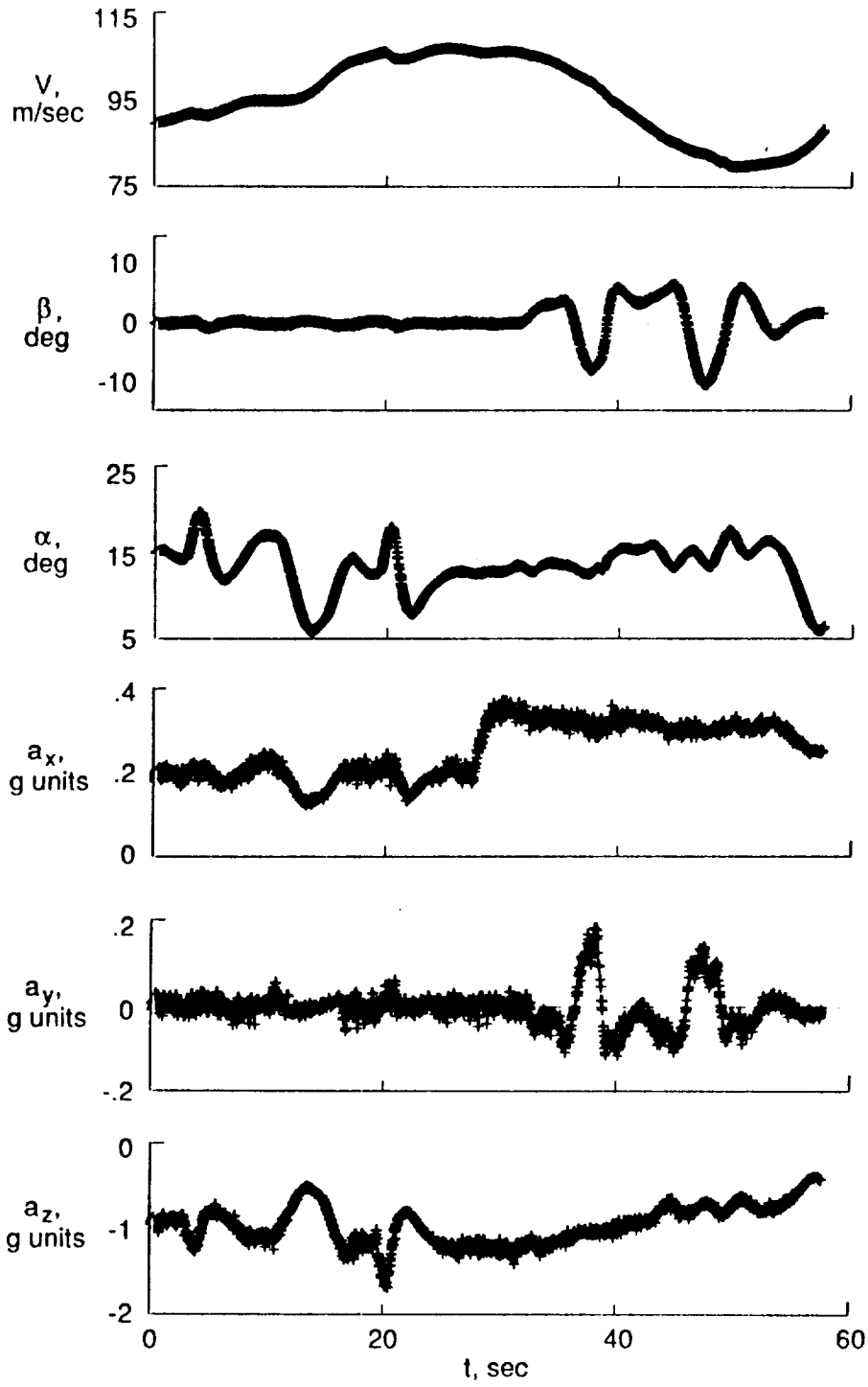

Figure 3. Continued.

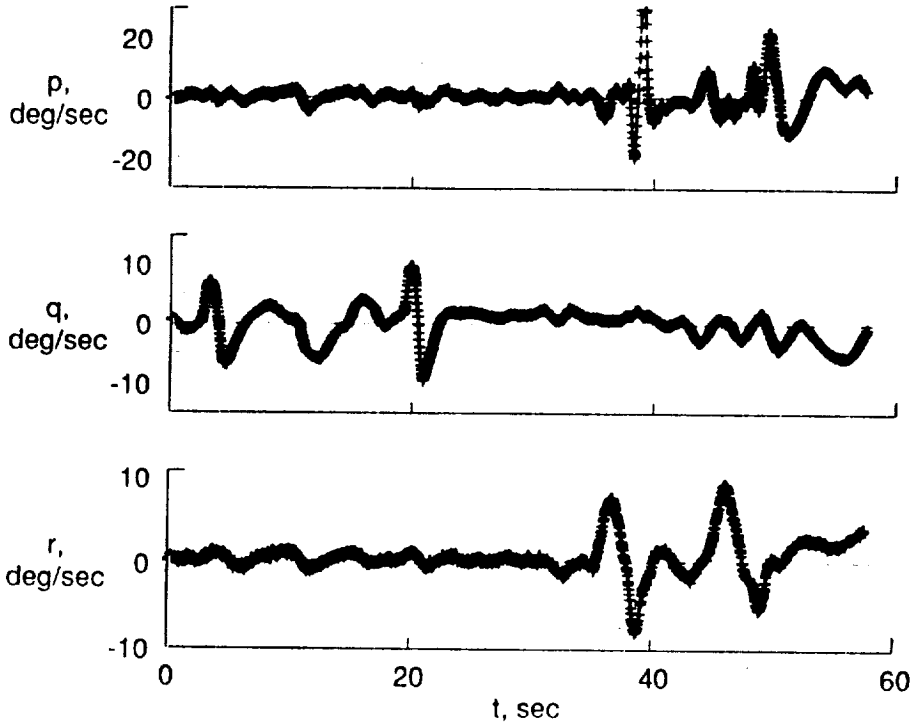

Figure 3. Concluded.

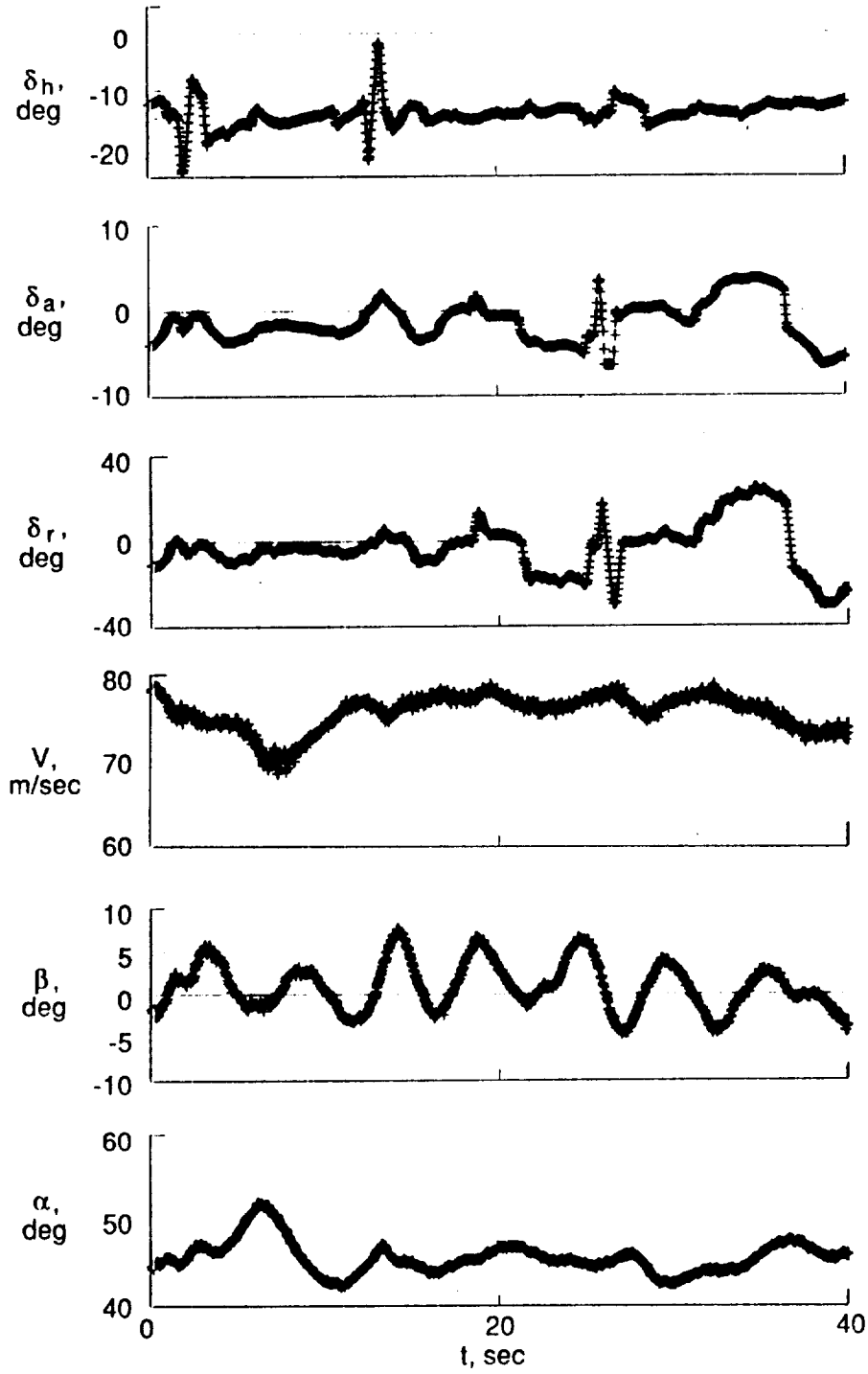

Figure 4. Time histories of measured input and response variables in small amplitude longitudinal and lateral maneuver ($\alpha \approx 44^{O}$).

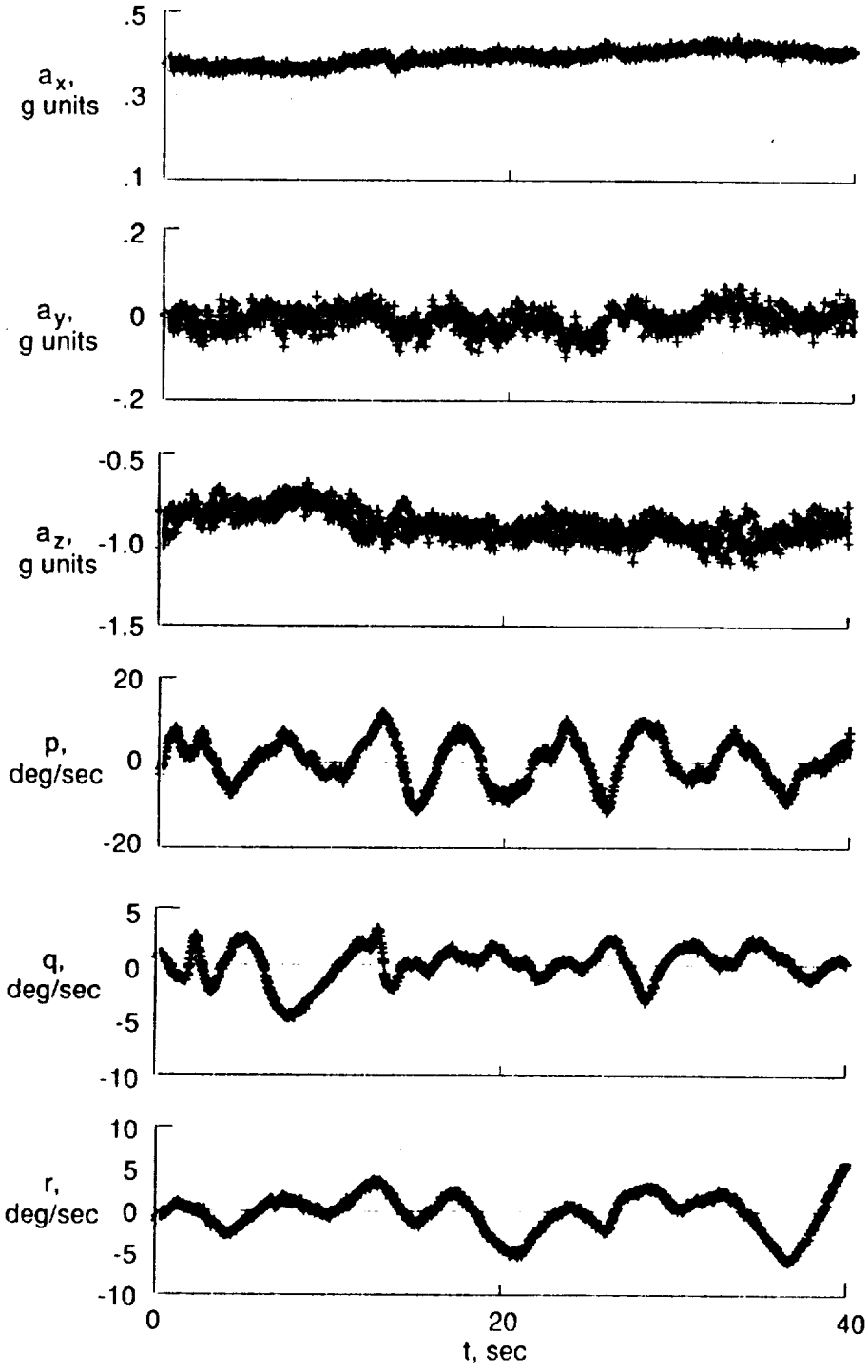

Figure 4. Concluded.

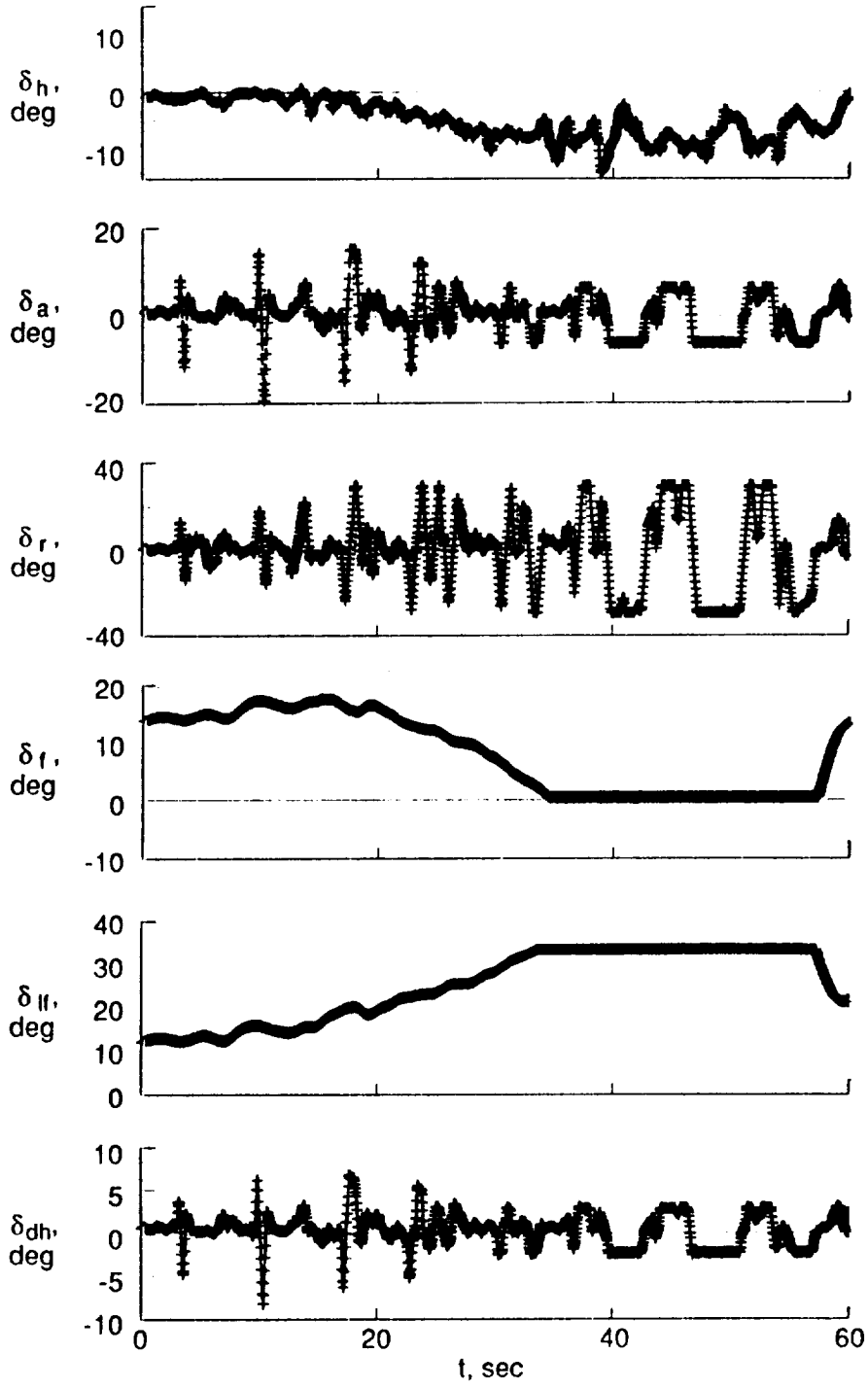

Figure 5. Time histories of measured input and response variables in large amplitude lateral maneuver.

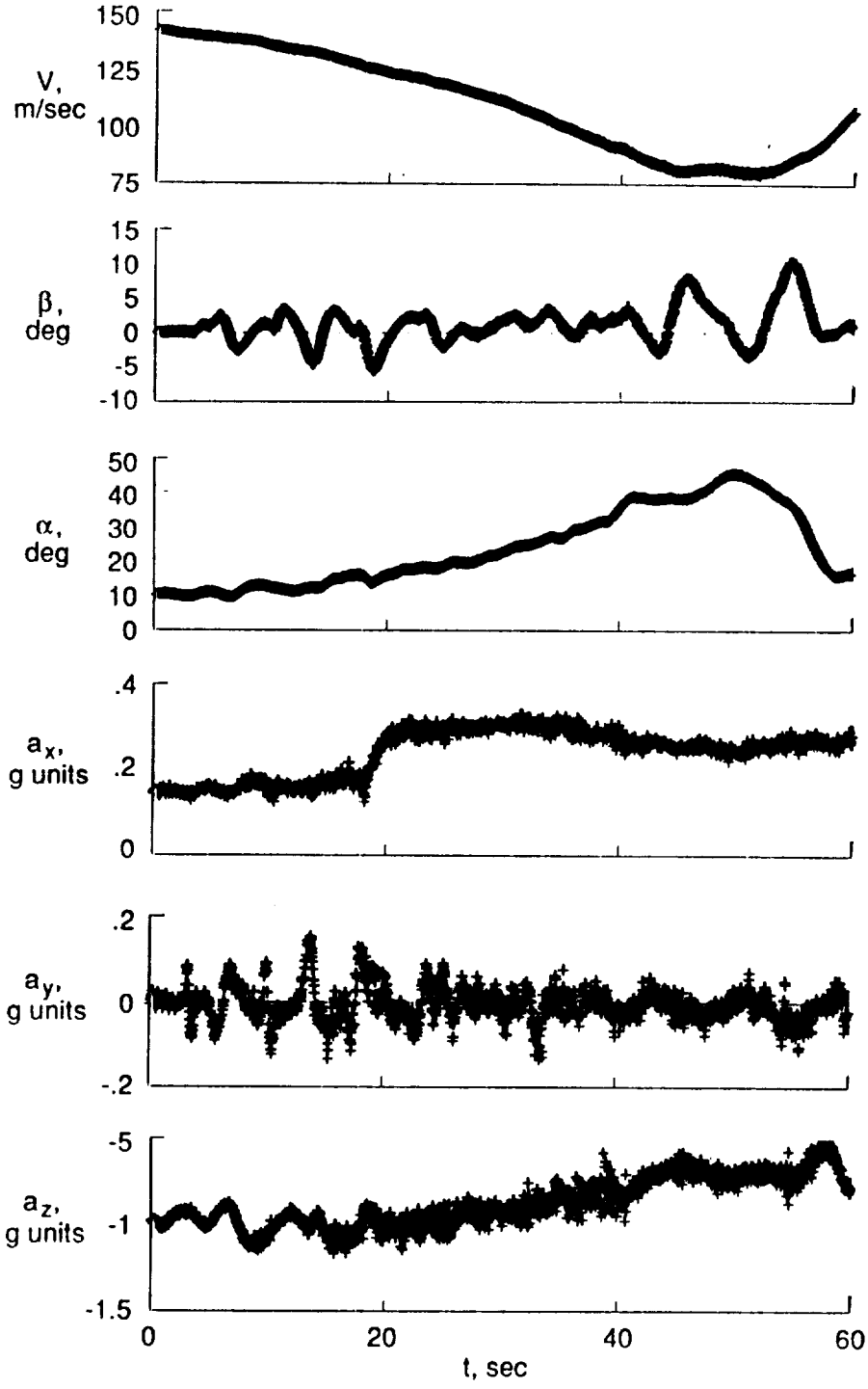

Figure 5. Continued.

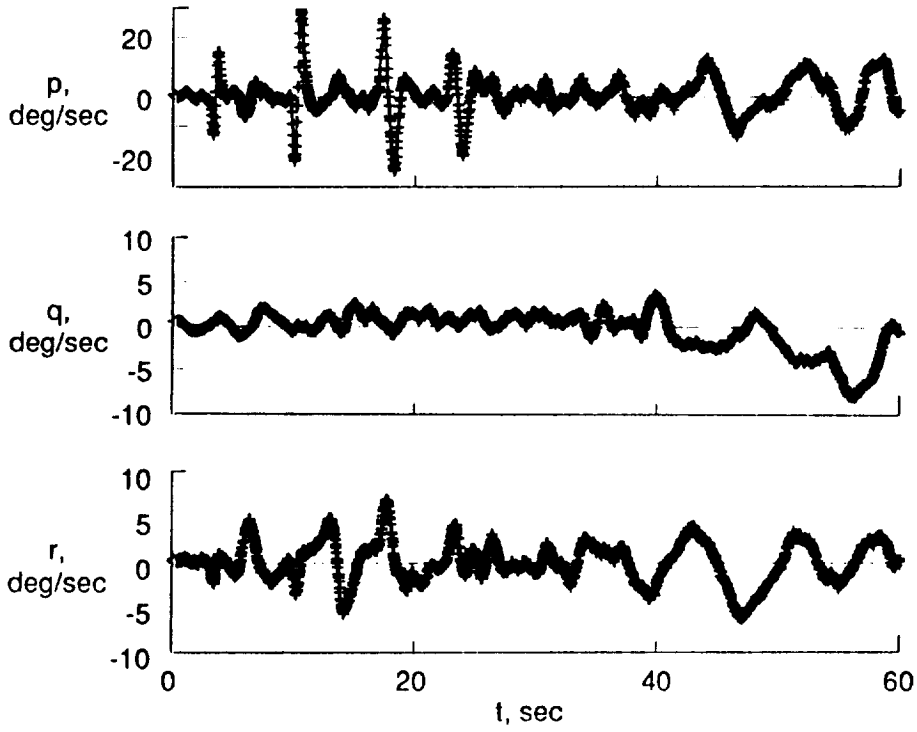

Figure 5. Concluded.

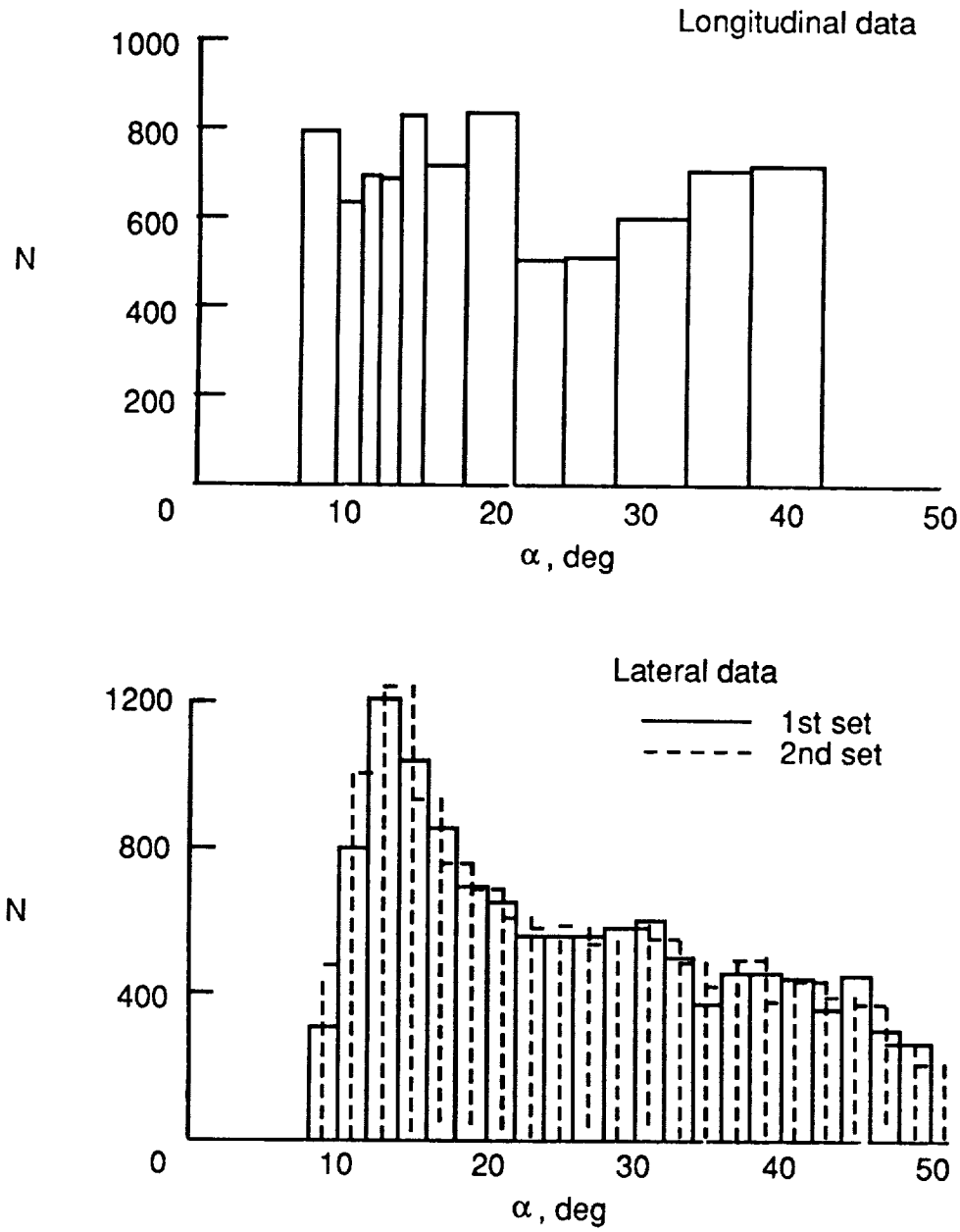

Figure 6. Number of data points in subsets using partitioning of data from large amplitude longitudinal and lateral maneuvers.

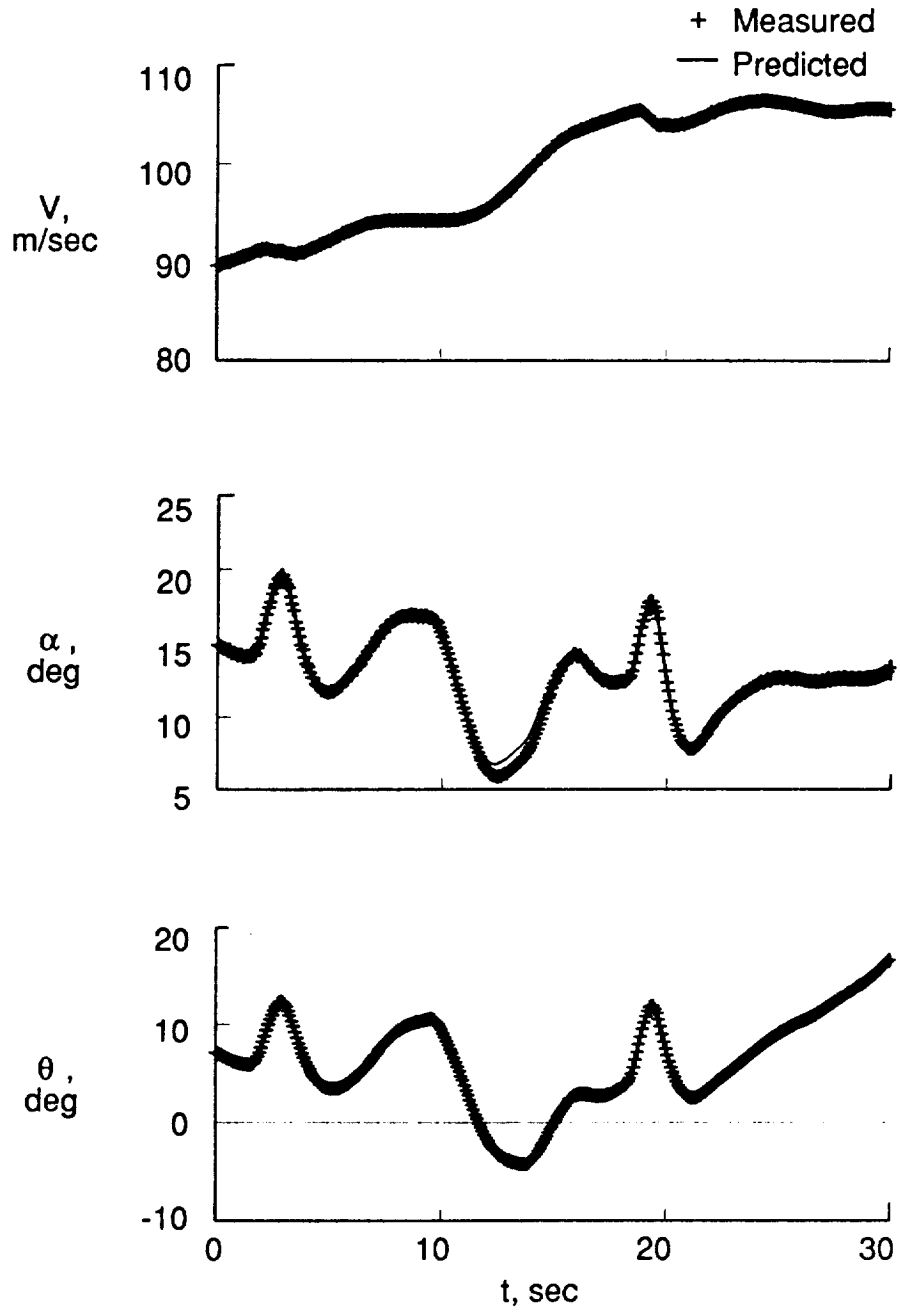

Figure 7. Comparison of measured and predicted longitudinal time histories in data compatibility check.

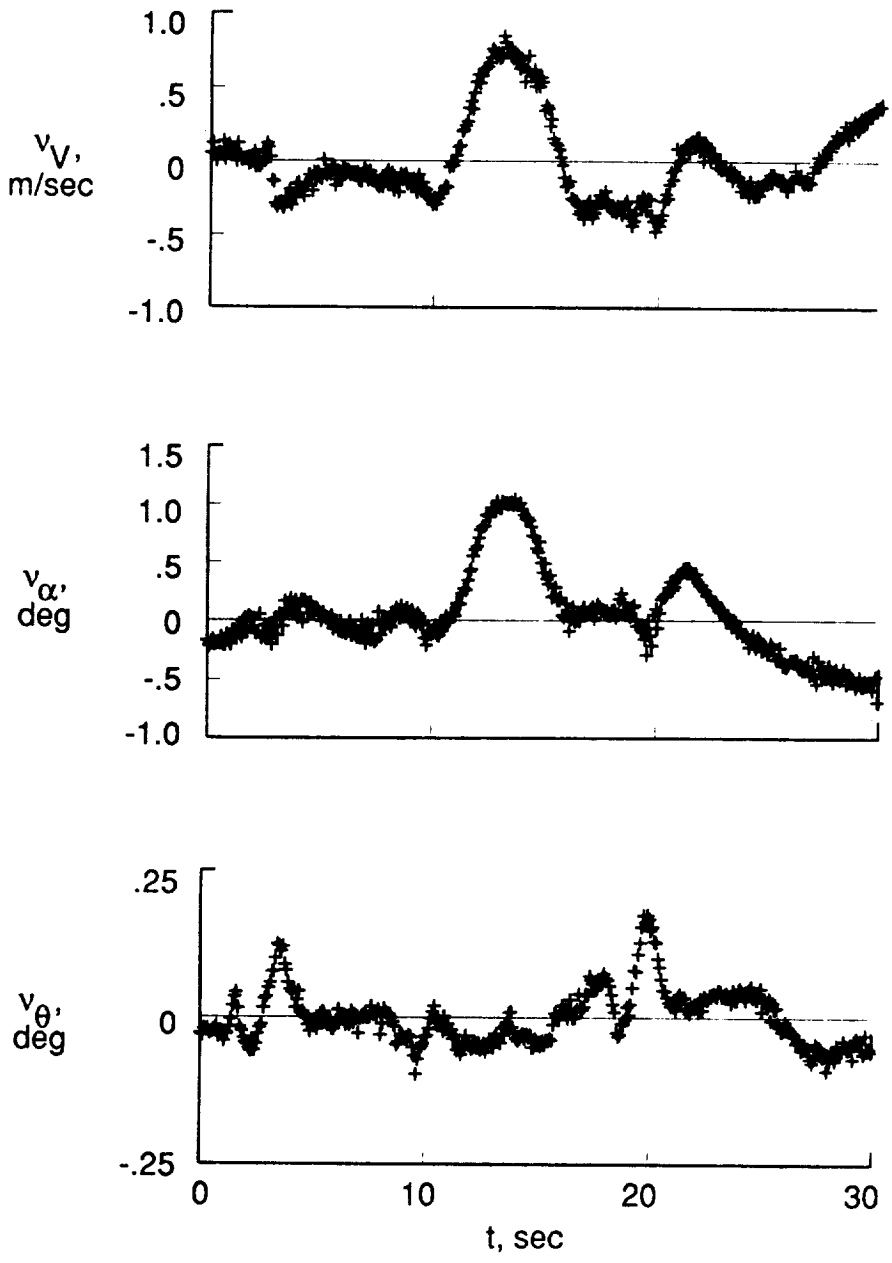

Figure 7. Concluded.

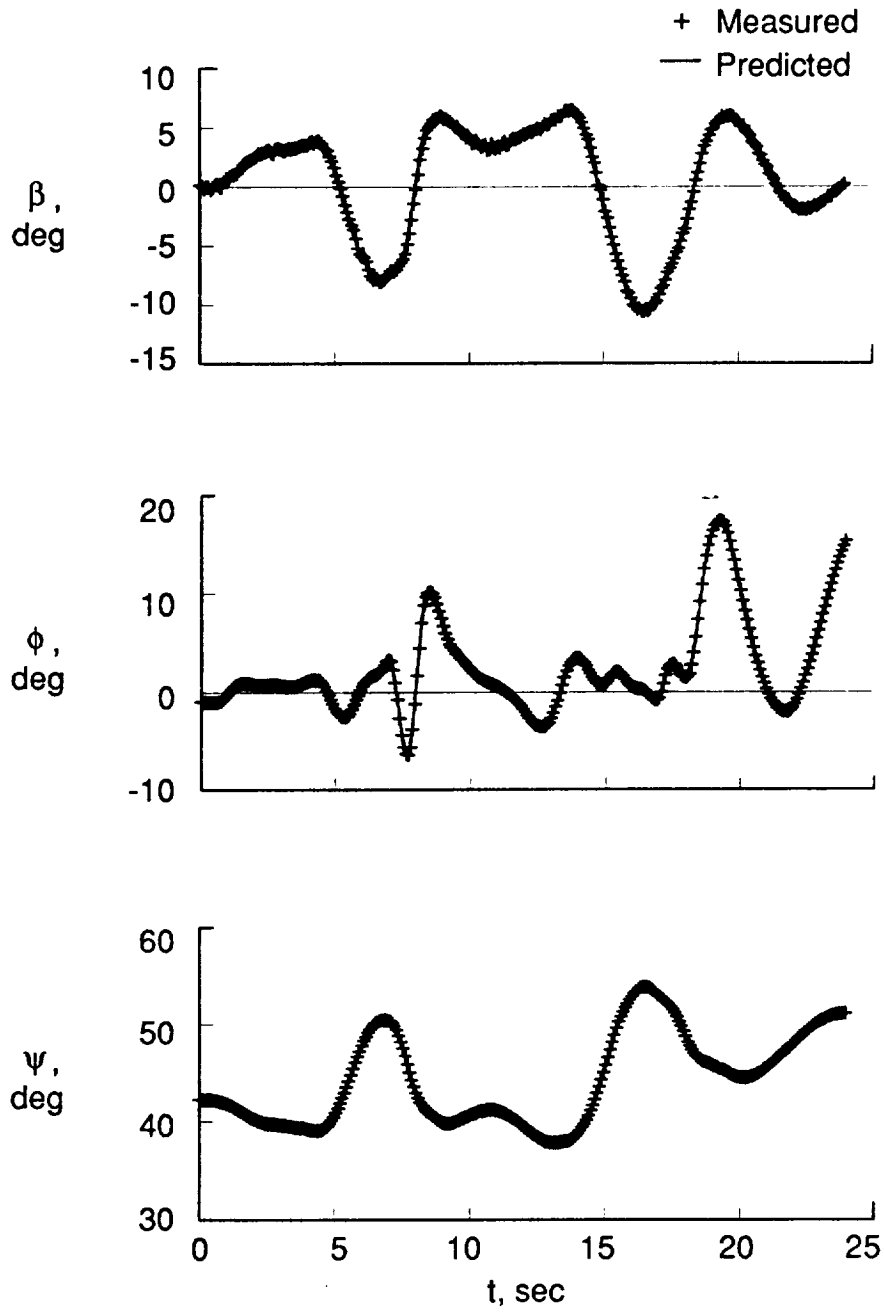

Figure 8. Comparison of measured and predicted lateral time histories in data compatibility check.

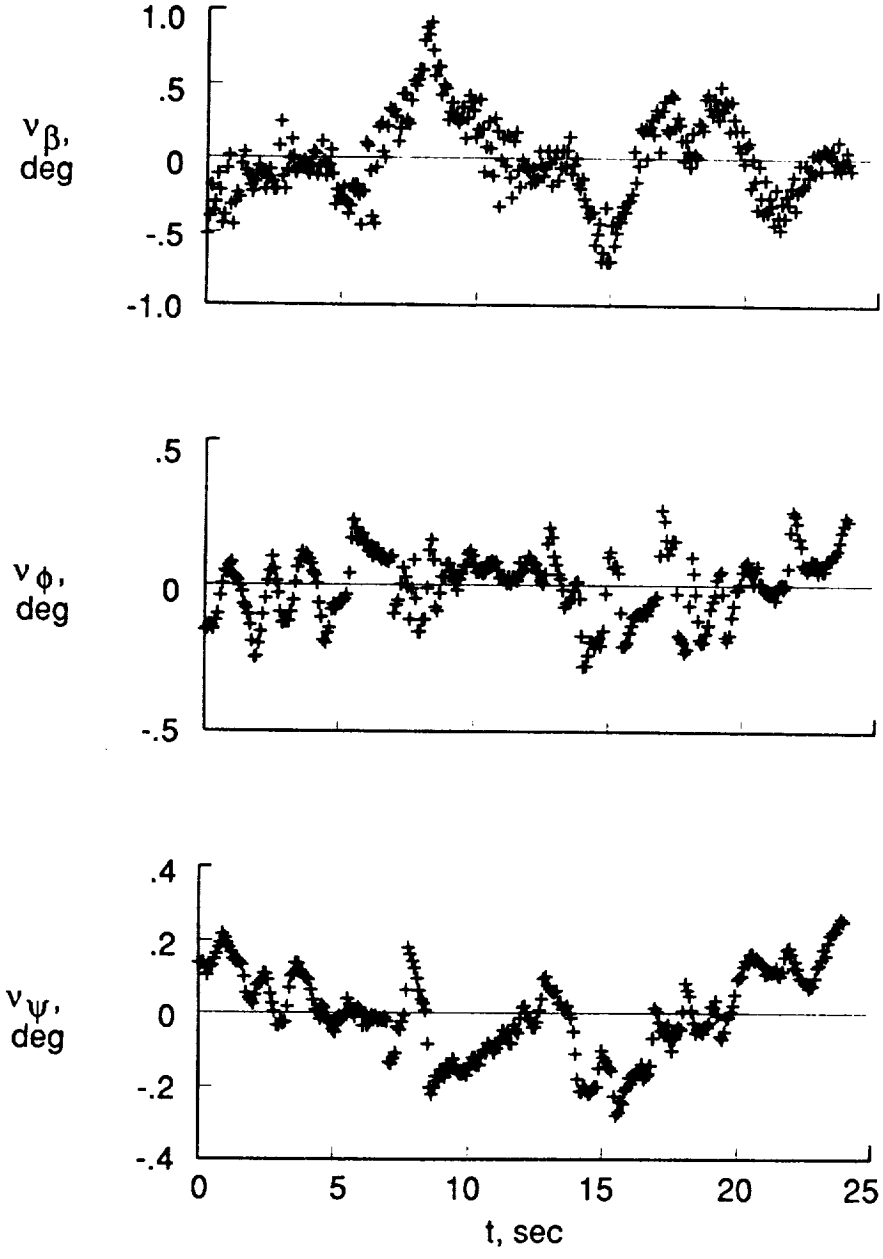

Figure 8. Concluded.

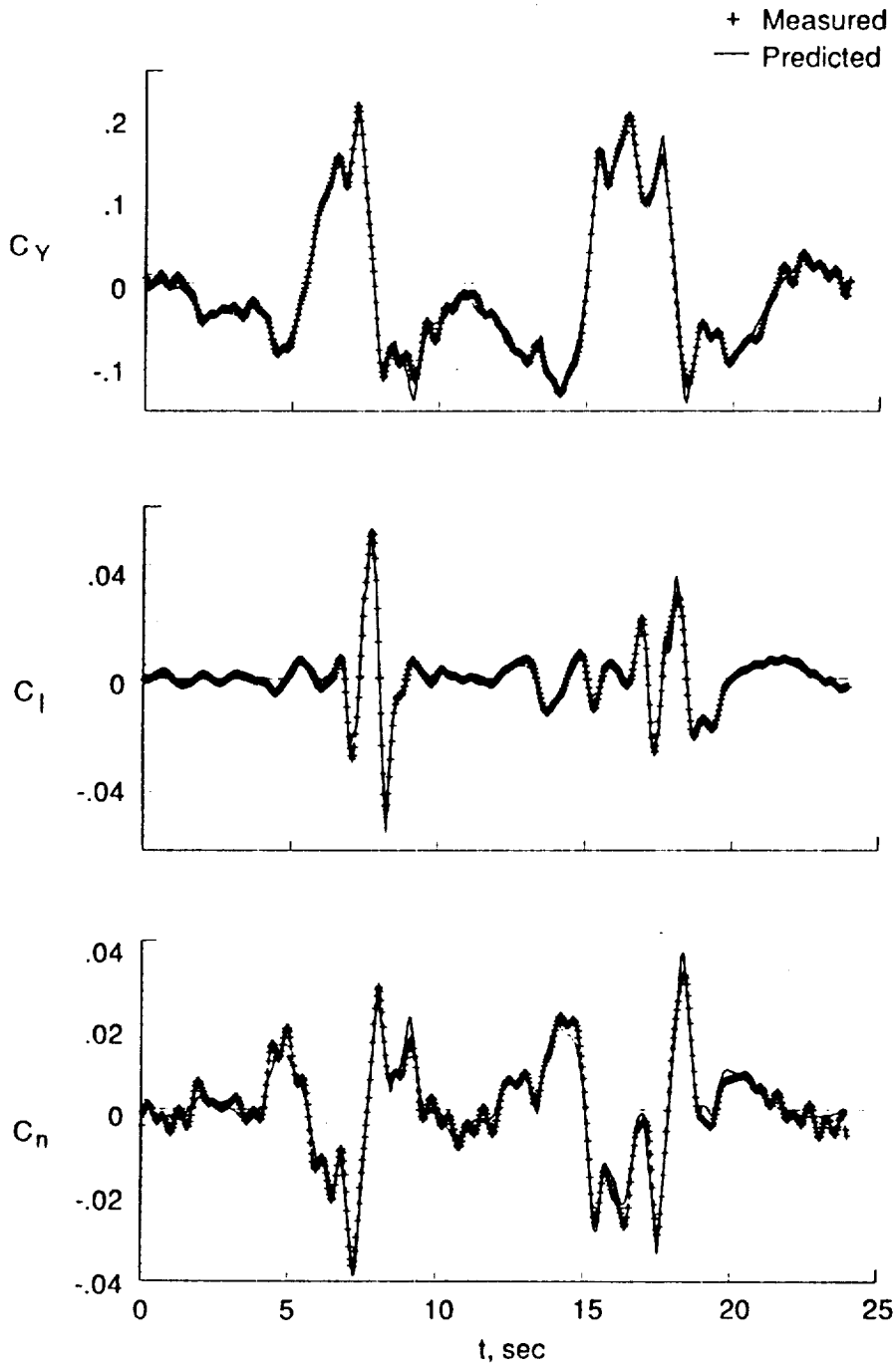

Figure 9. Time histories of measured and predicted lateral coefficients and corresponding residuals.

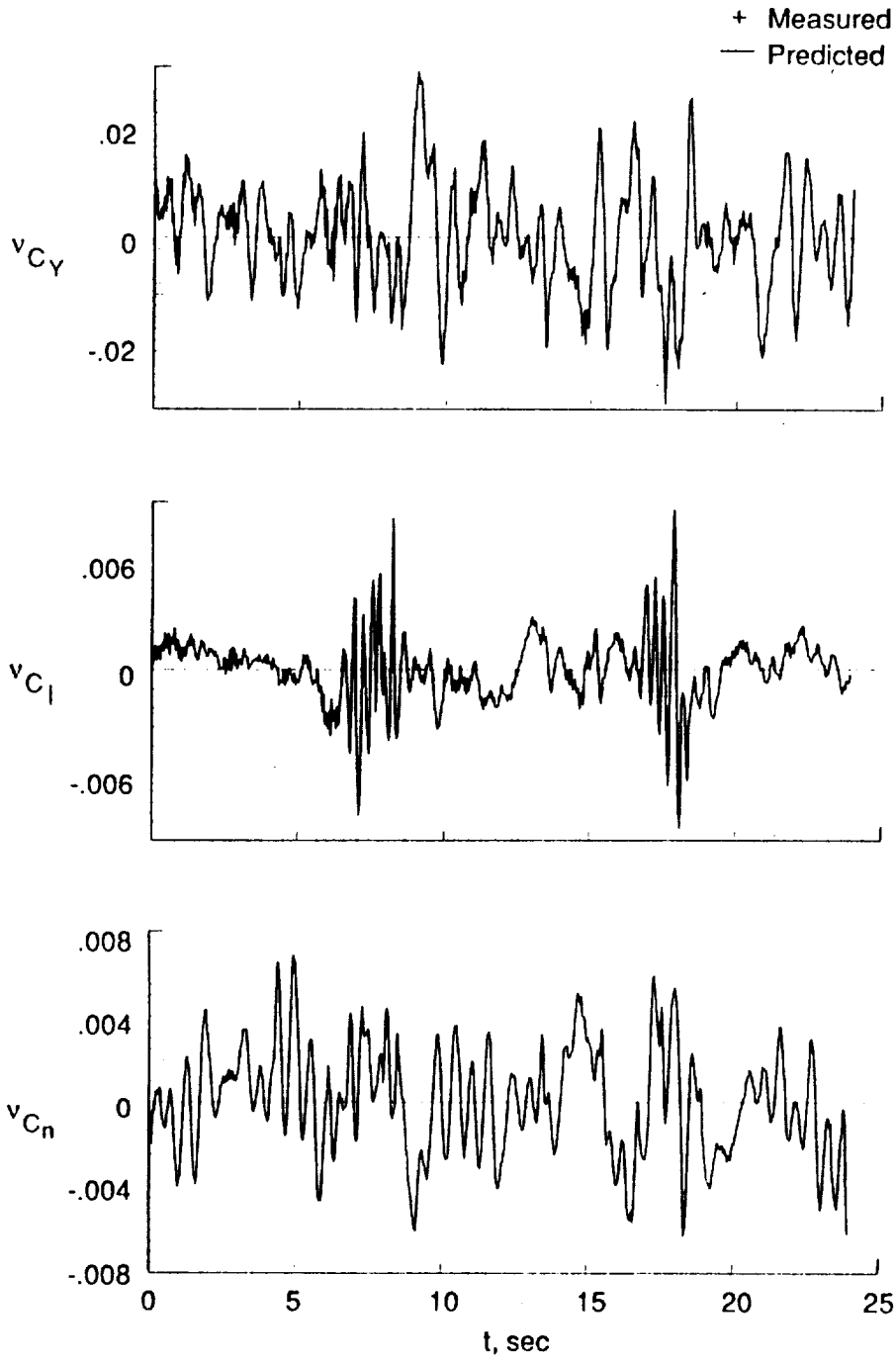

Figure 9. Concluded.

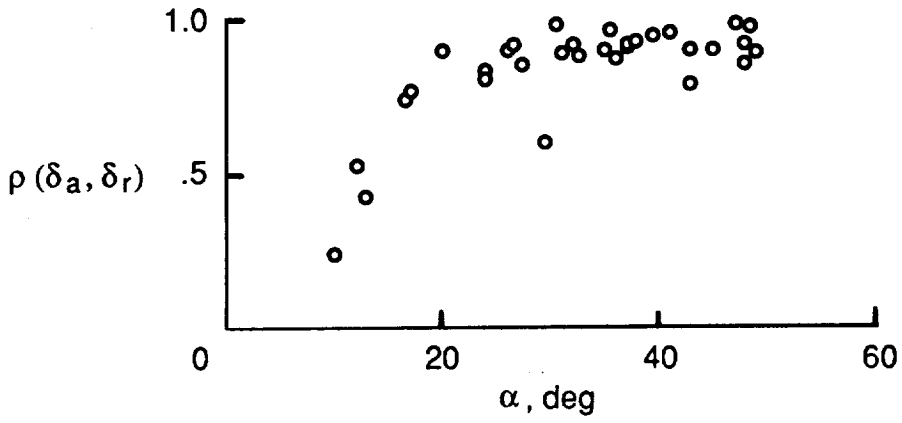

Figure 10. Variation of correlation between aileron and rudder deflection with the angle of attack.

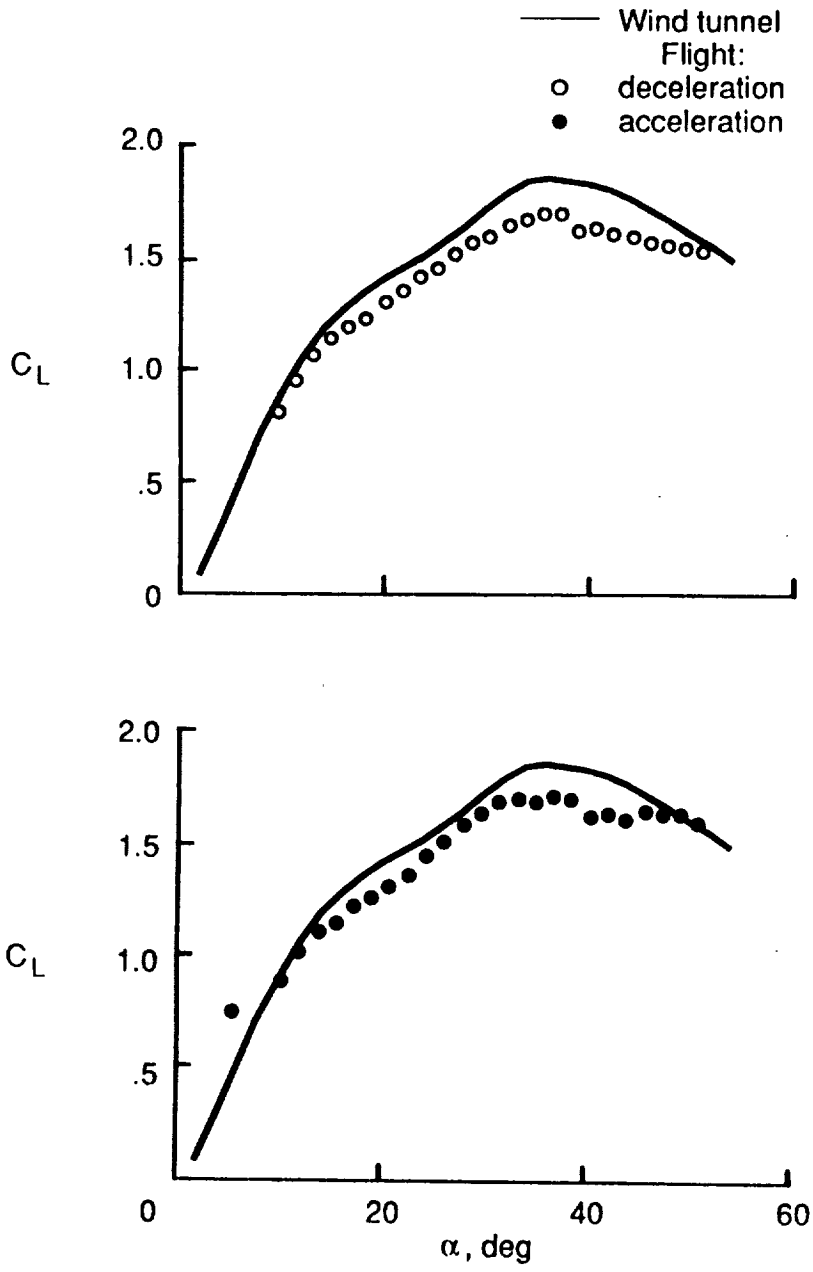

Figure 11. Comparison of lift coefficient at steady conditions estimated from deceleration/acceleration maneuver and wind tunnel data. Scheduled flaps, $\delta_h = -6^o$.

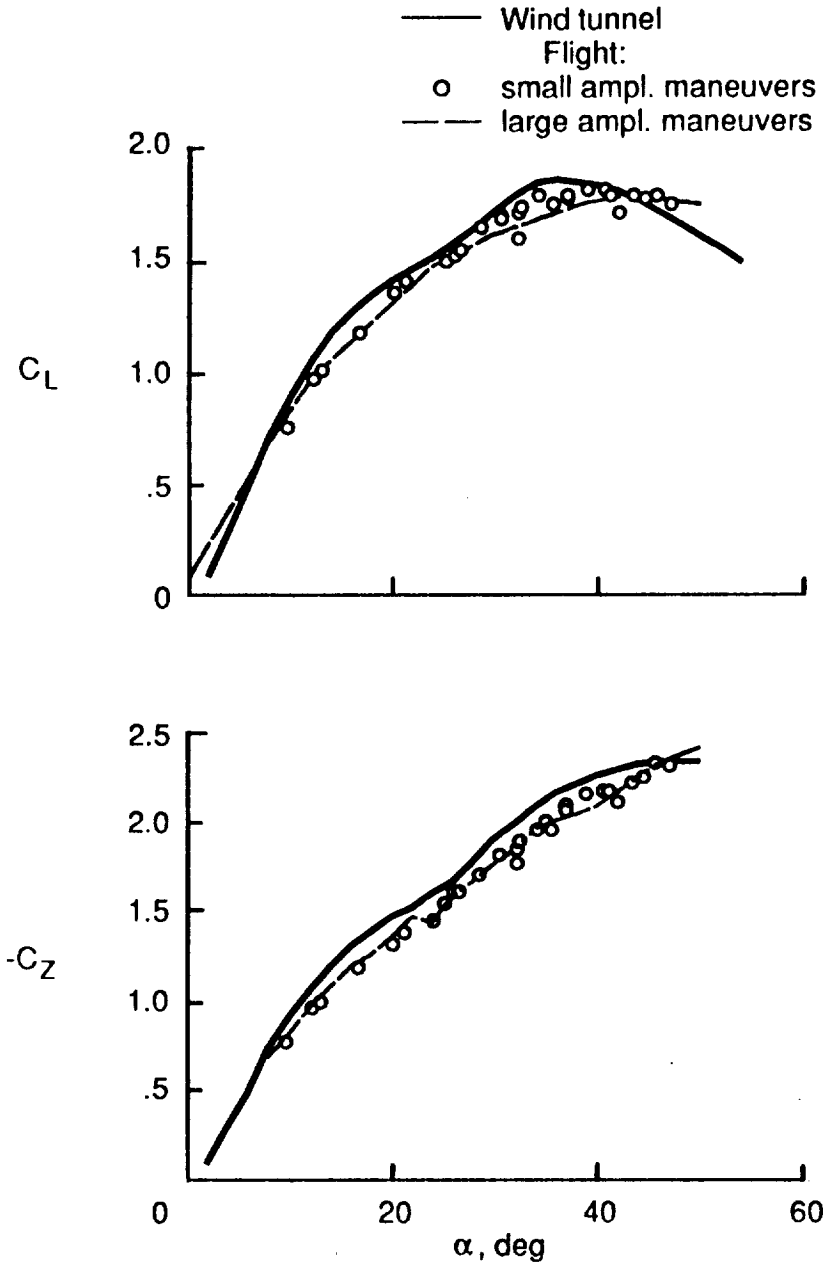

Figure 12. Comparison of lift and vertical-force coefficient at steady conditions estimated from flight and wind tunnel data. Scheduled flaps, $\delta_h = -6^o$.

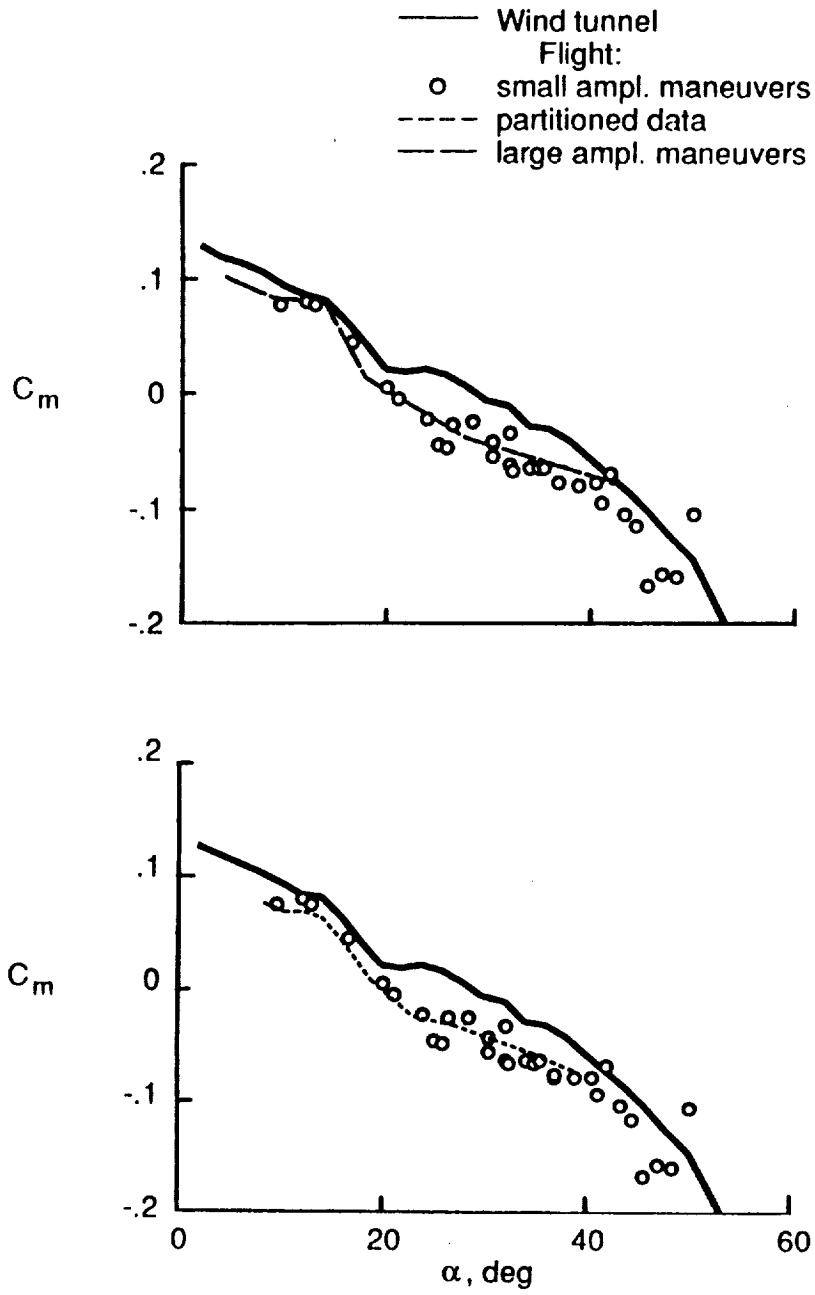

Figure 13. Comparison of pitching-moment coefficient at steady conditions estimated from flight and wind tunnel data. Scheduled flaps, $\delta_h = -6^o$.

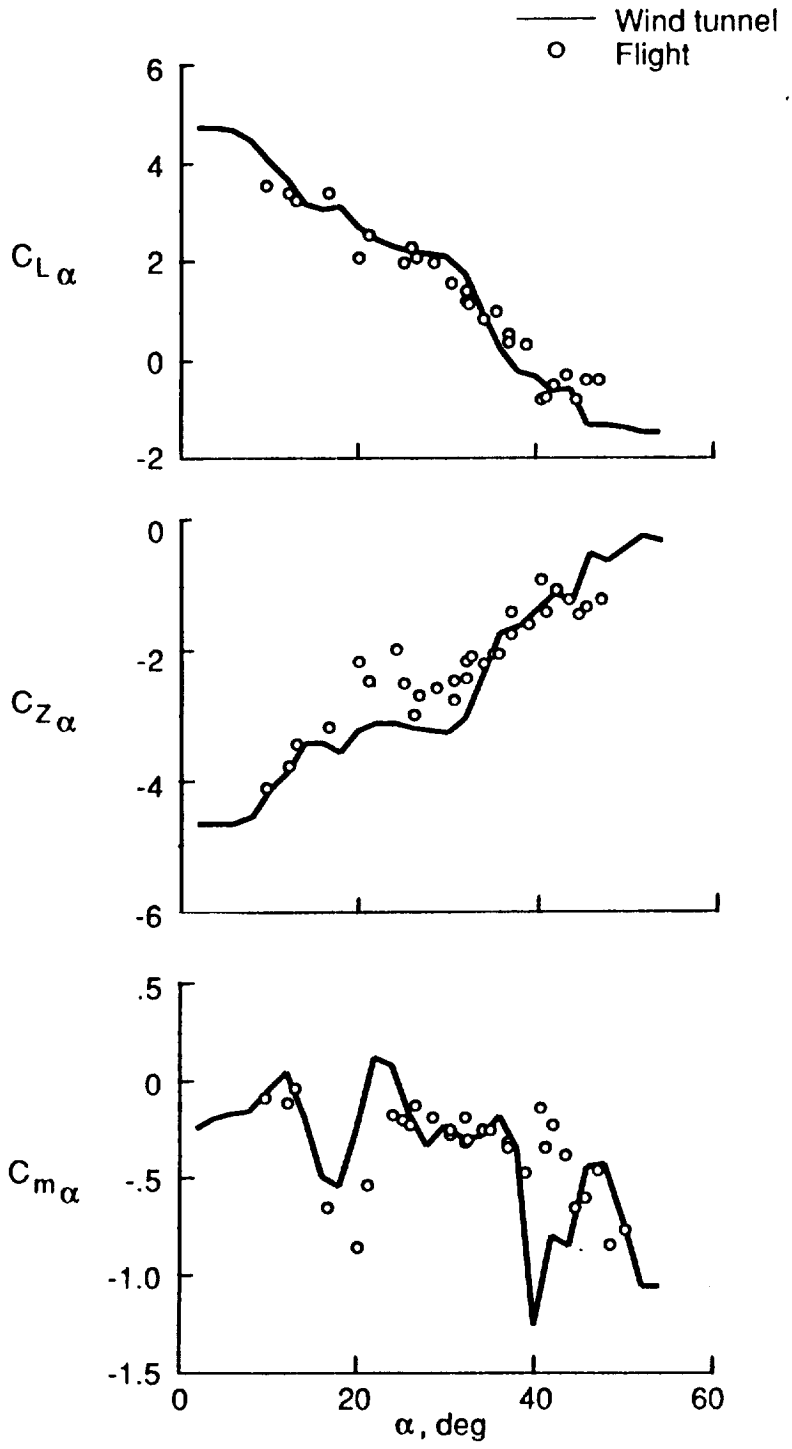

Figure 14. Comparison of longitudinal stability parameters estimated from small amplitude maneuvers and wind tunnel measurement.

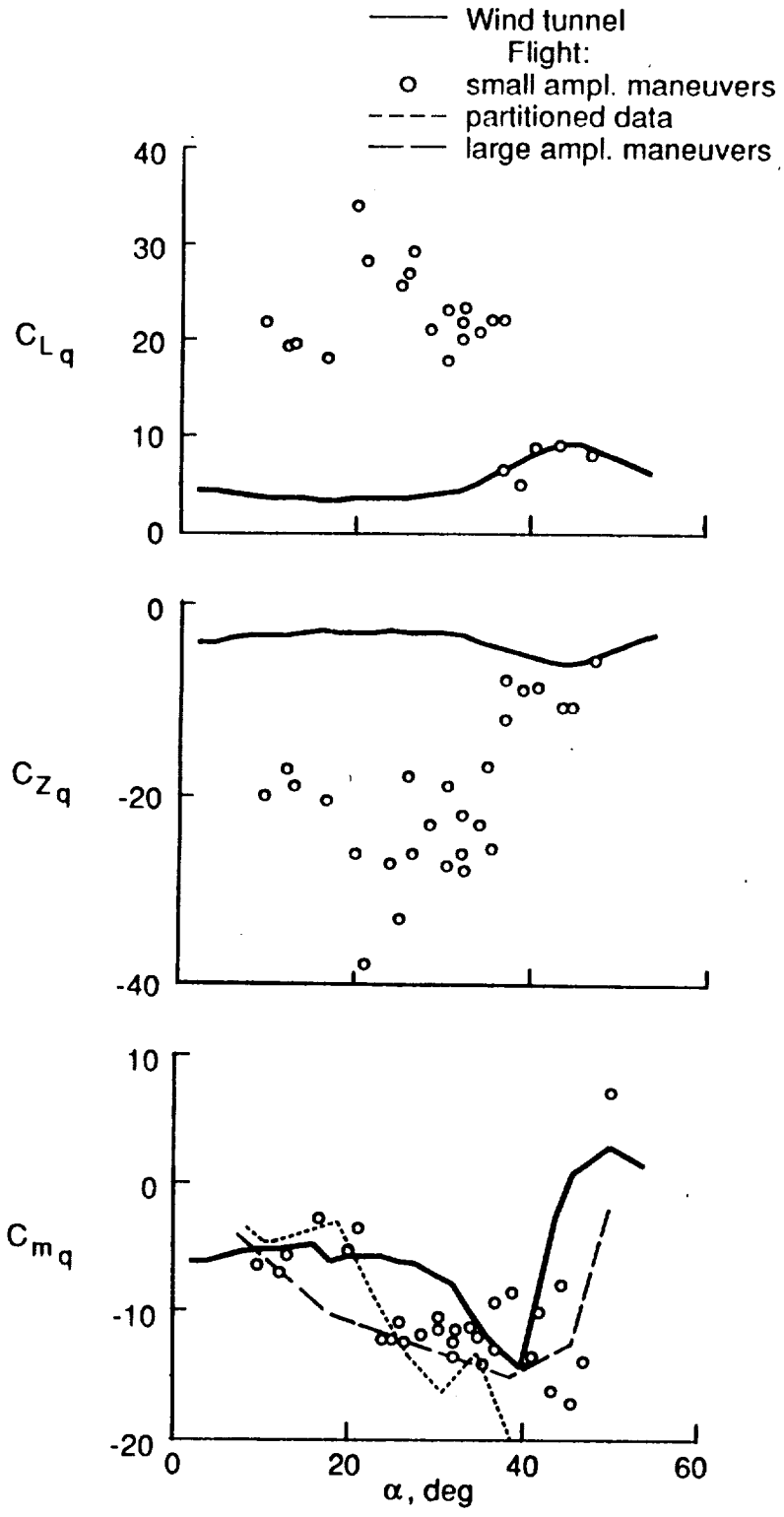

Figure 15. Comparison of pitch-rate parameters estimated from flight and wind tunnel data.

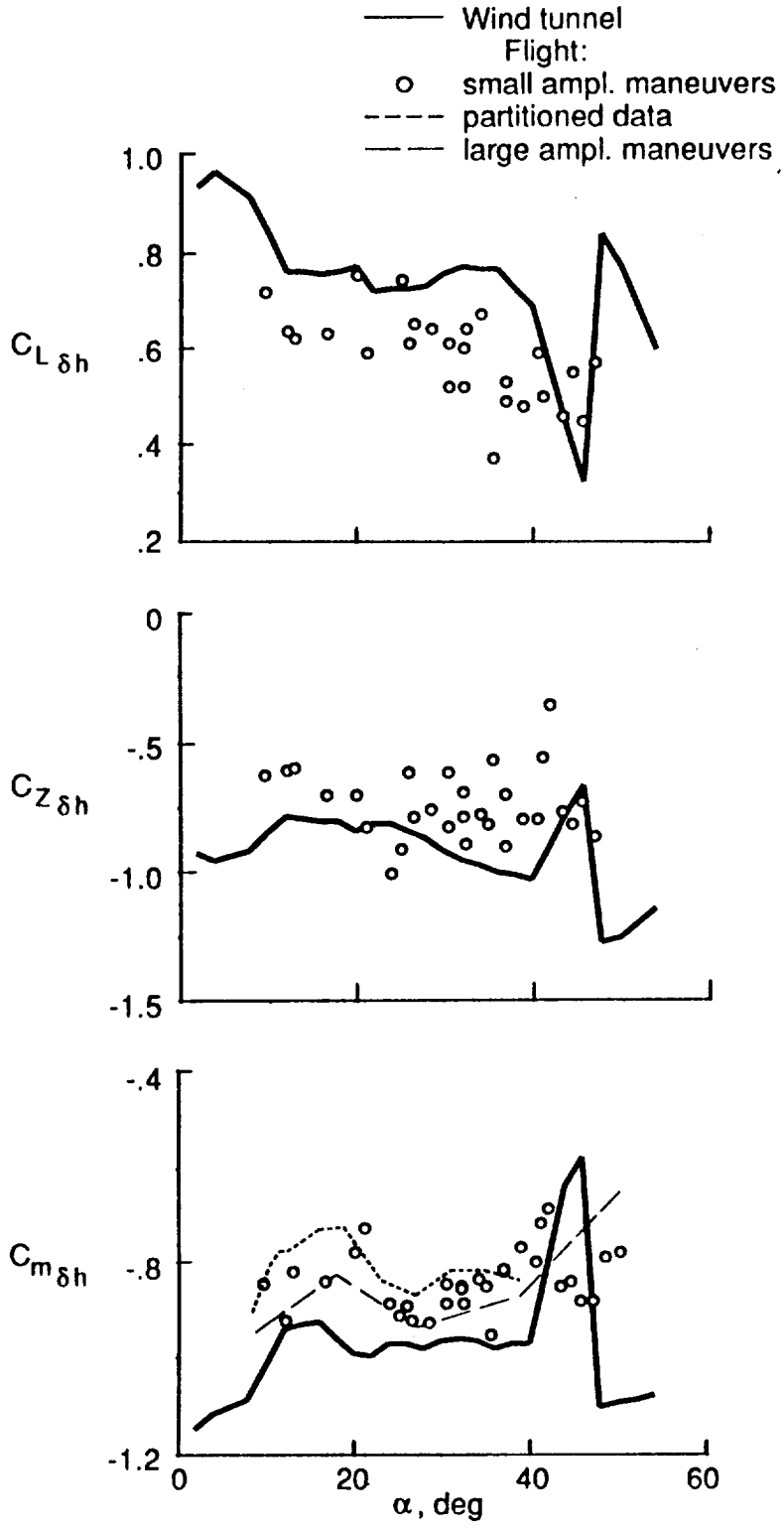

Figure 16. Comparison of longitudinal control parameters estimated from flight and wind tunnel data.

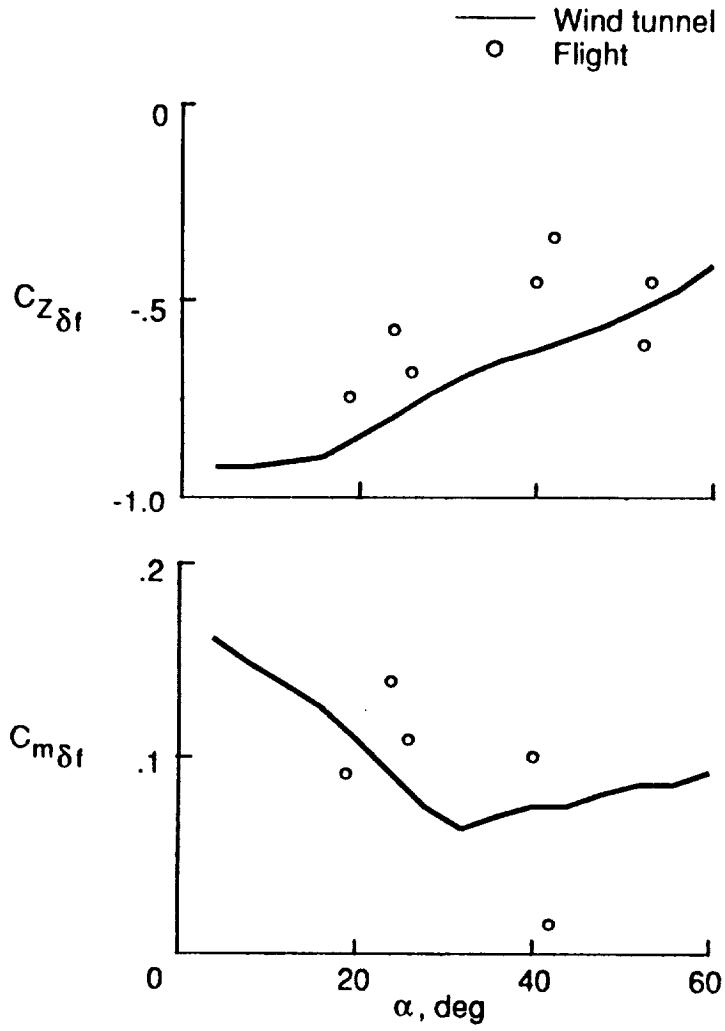

Figure 17. Comparison of parameters expressing trailing-edge flaps effect estimated from small amplitude maneuvers and wind tunnel measurement.

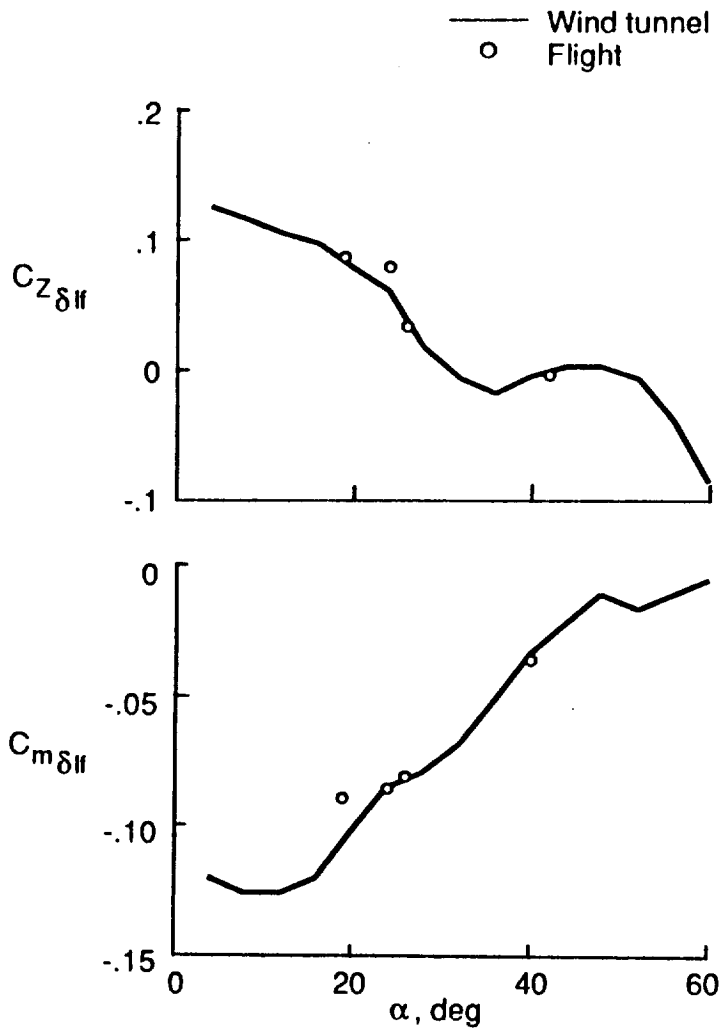

Figure 18. Comparison of parameters expressing leading-edge flaps effect estimated from small amplitude maneuvers and wind tunnel measurement.

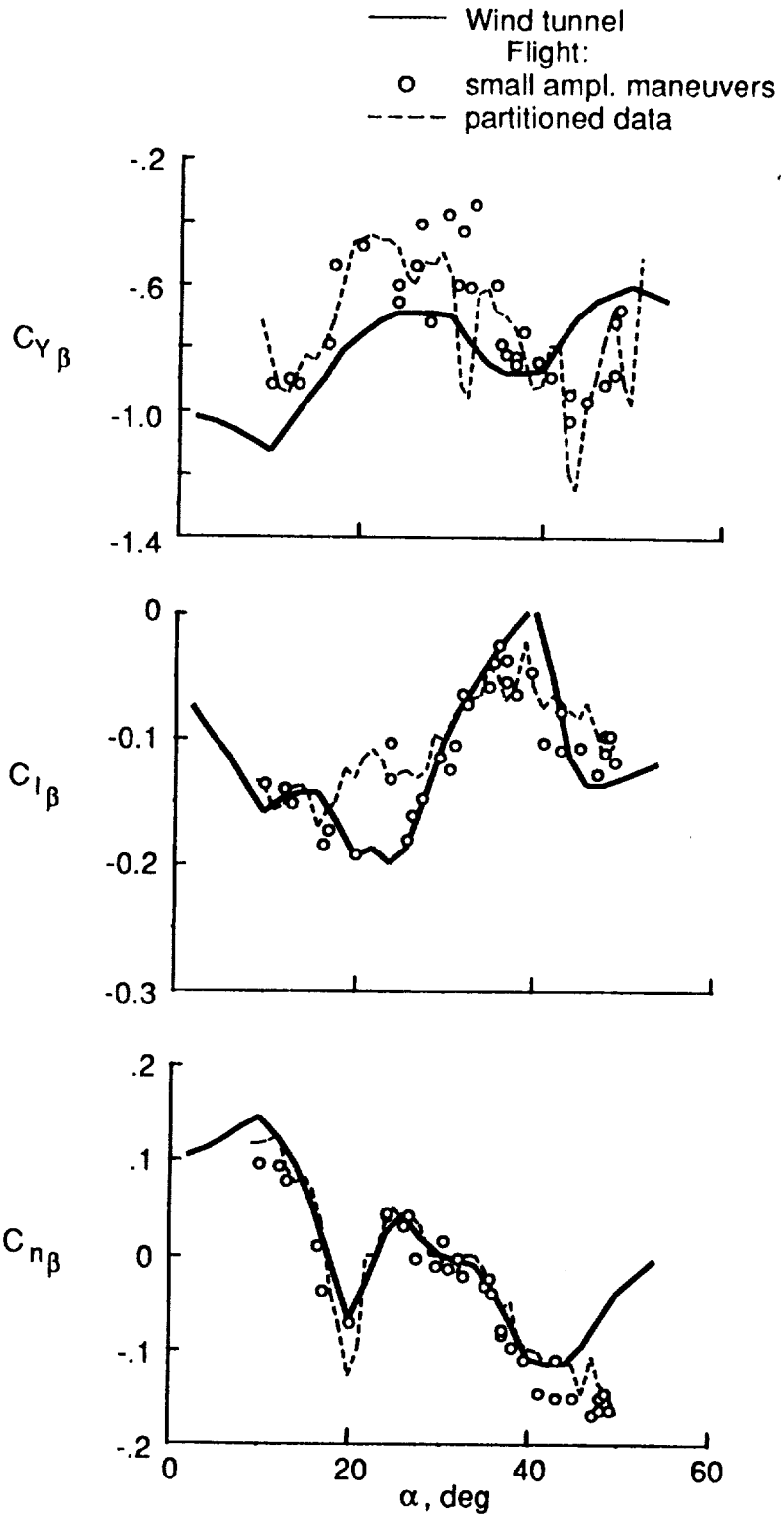

Figure 19. Comparison of sideslip parameters estimated from flight and wind tunnel data.

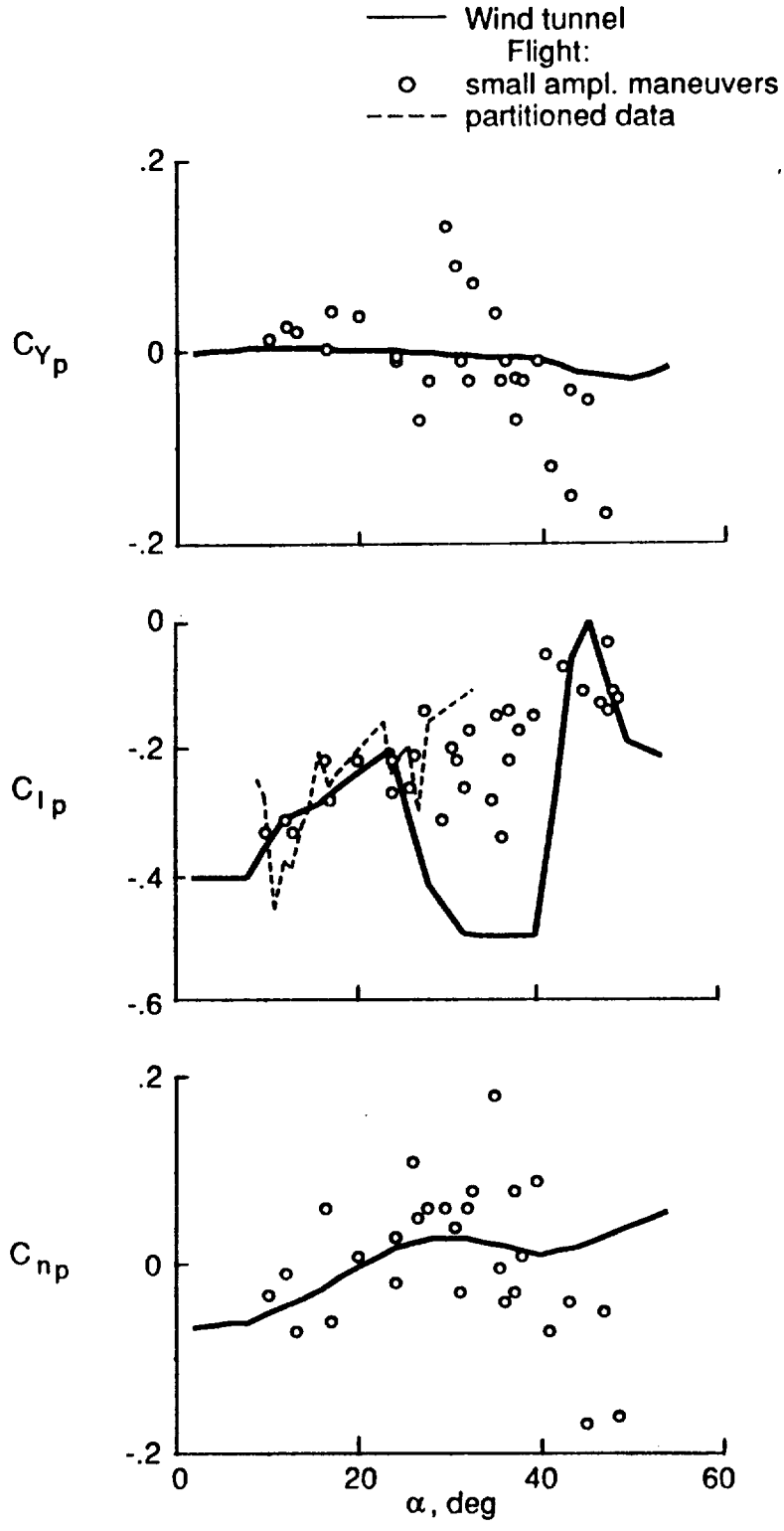

Figure 20. Comparison of roll-rate parameters estimated from flight and wind tunnel data.

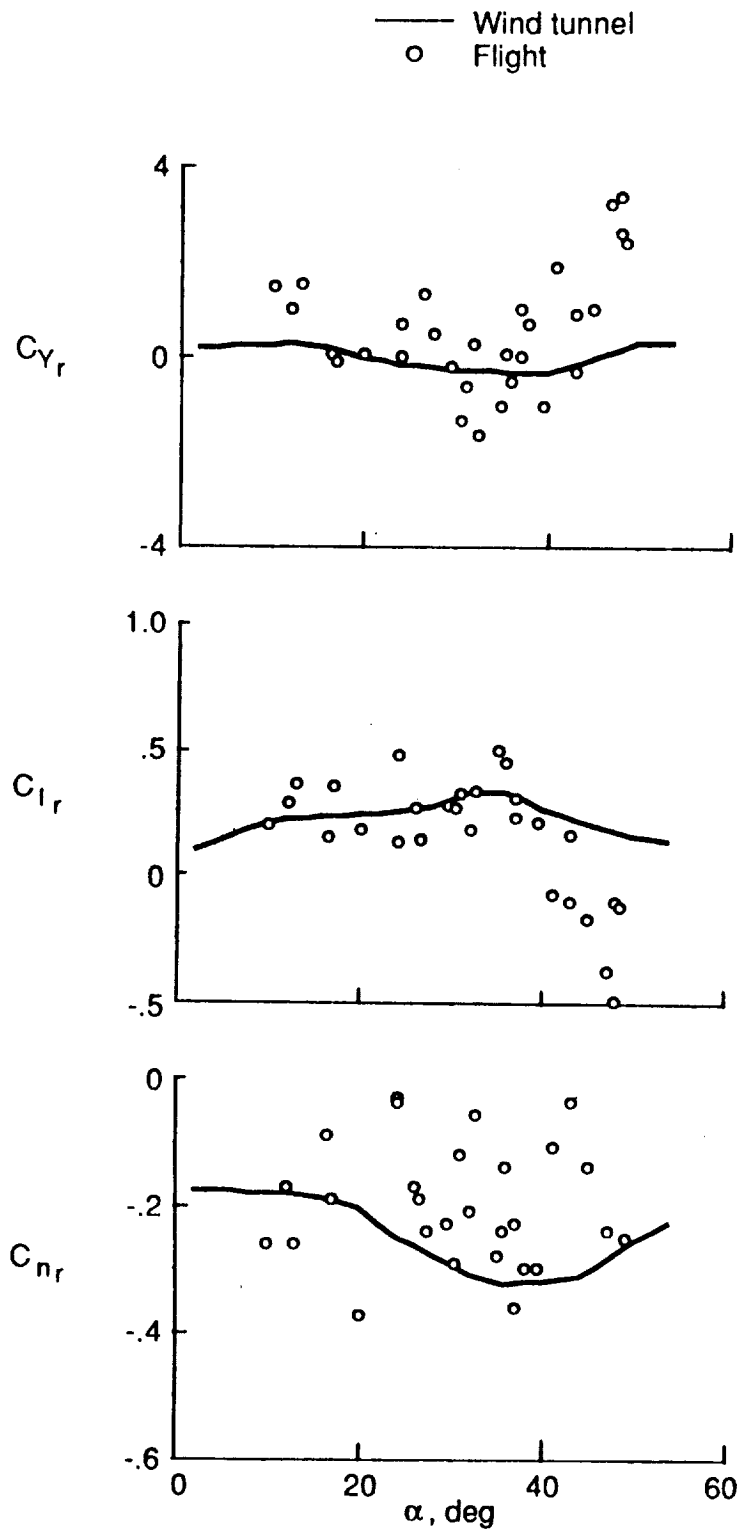

Figure 21. Comparison of yaw-rate parameters estimated from flight and wind tunnel data.

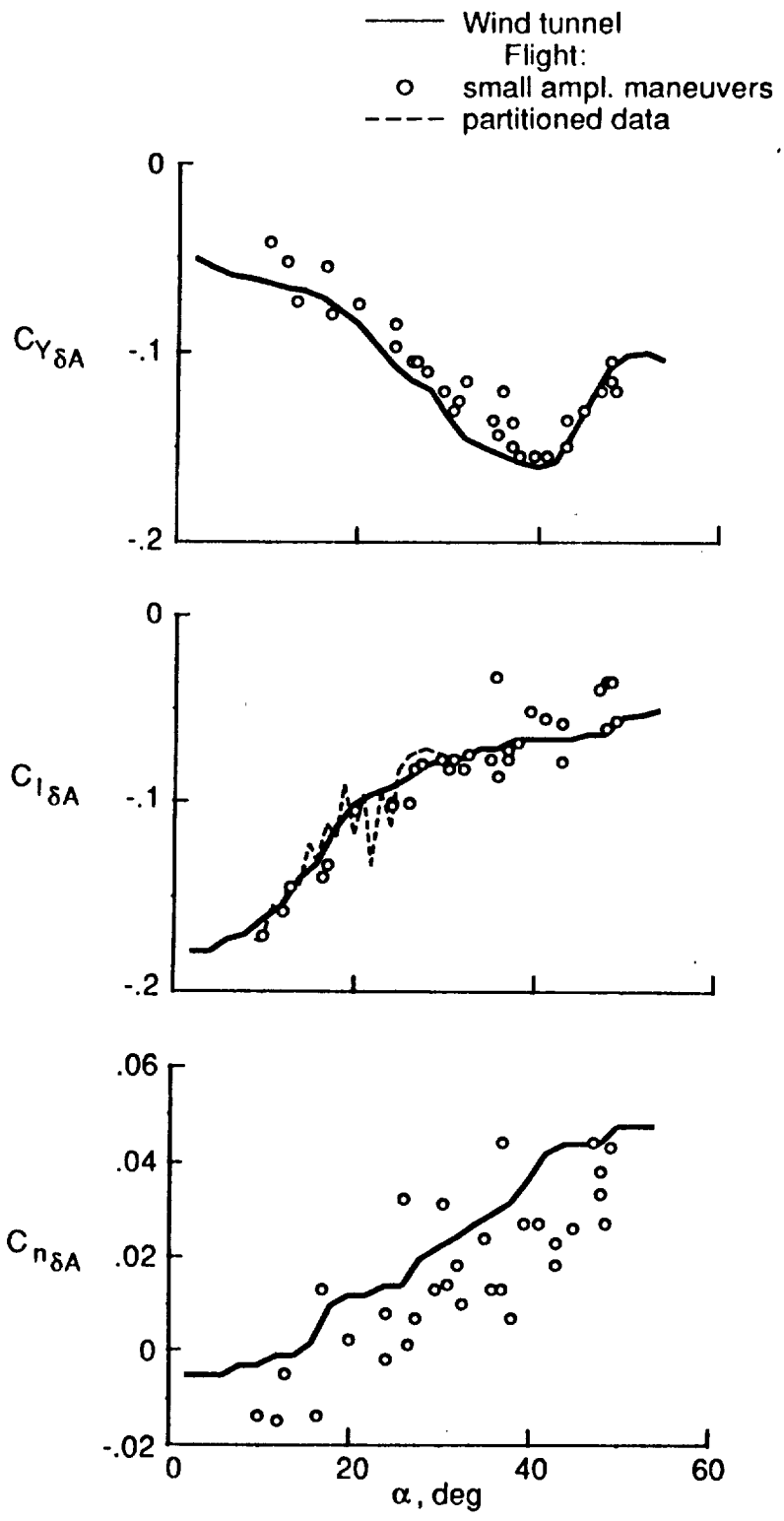

Figure 22. Comparison of aileron-effectiveness parameters estimated from flight and wind tunnel data.

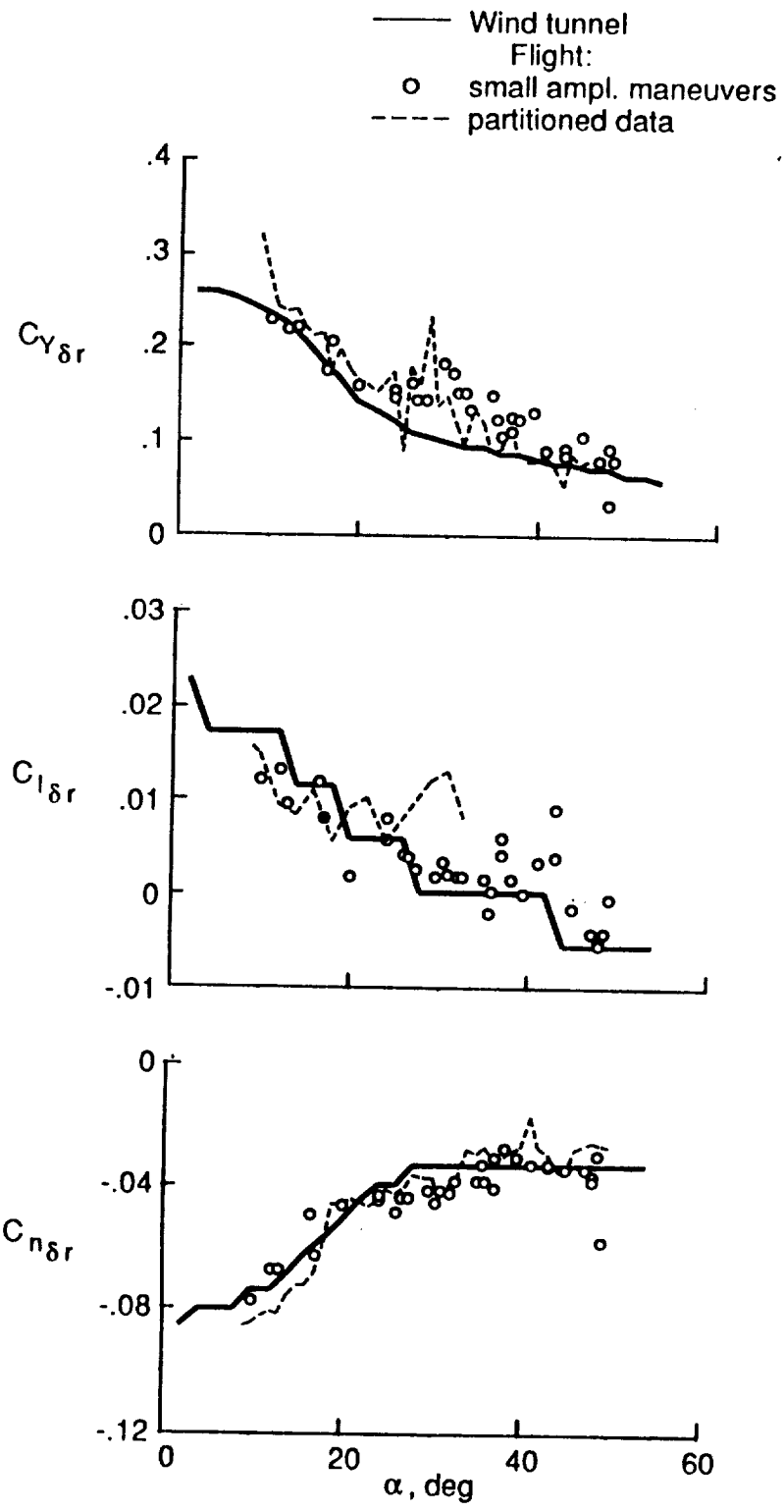

Figure 23. Comparison of rudder-effectiveness parameters estimated from flight and wind tunnel data.

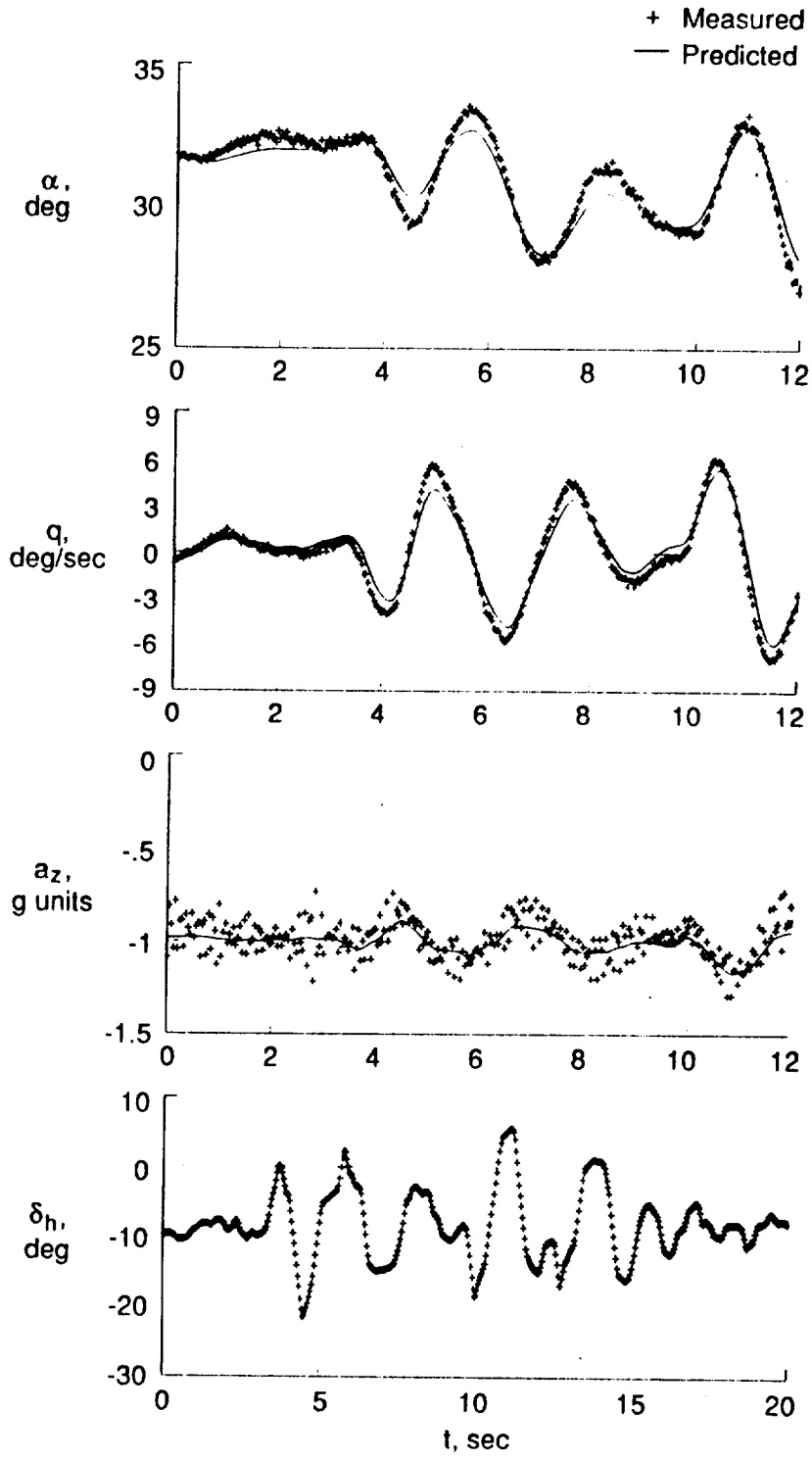

Figure 24. Comparison of measured longitudinal time histories with those computed.

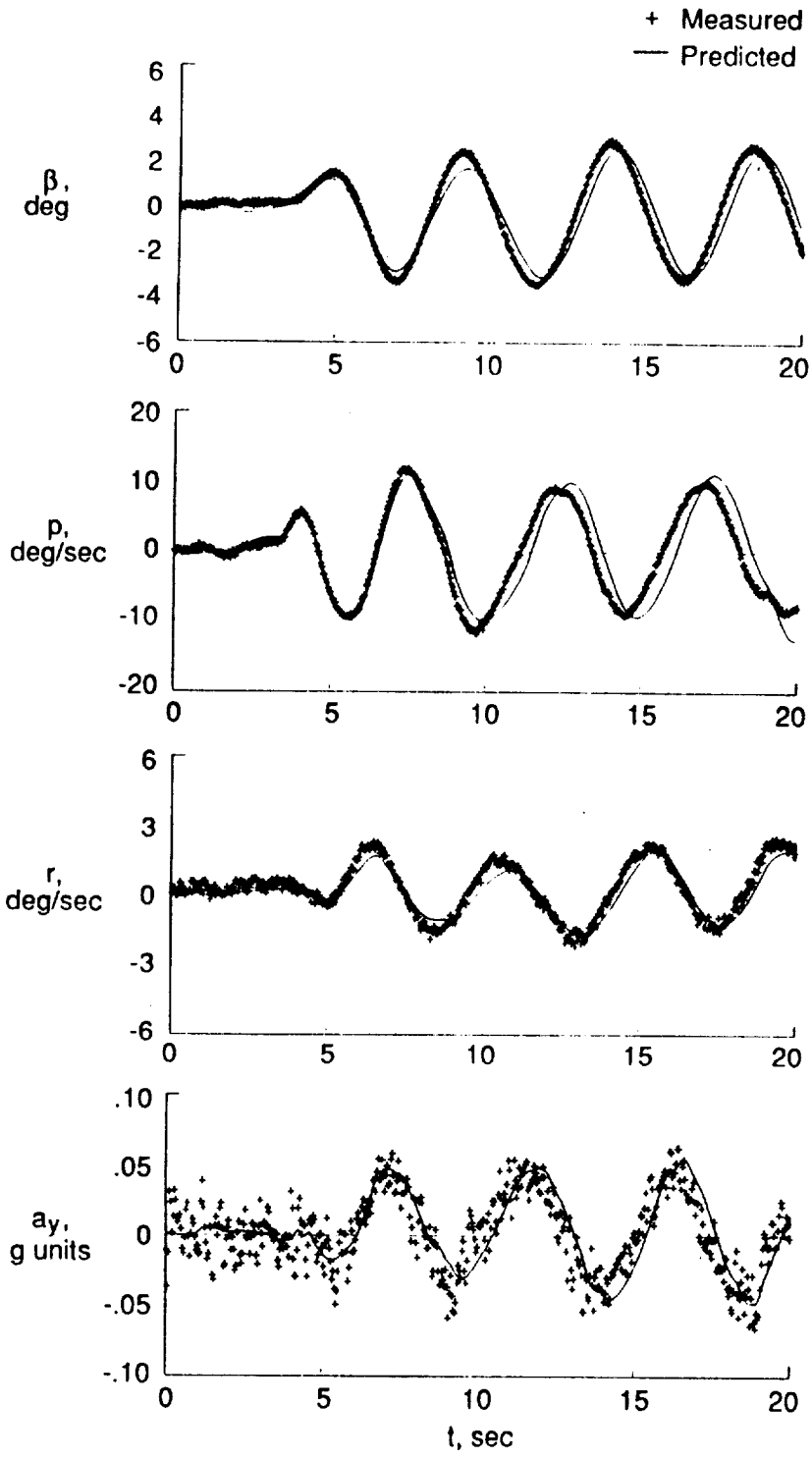

Figure 25. Comparison of measured lateral time histories with those computed. $\alpha_0 \approx 12^0$.

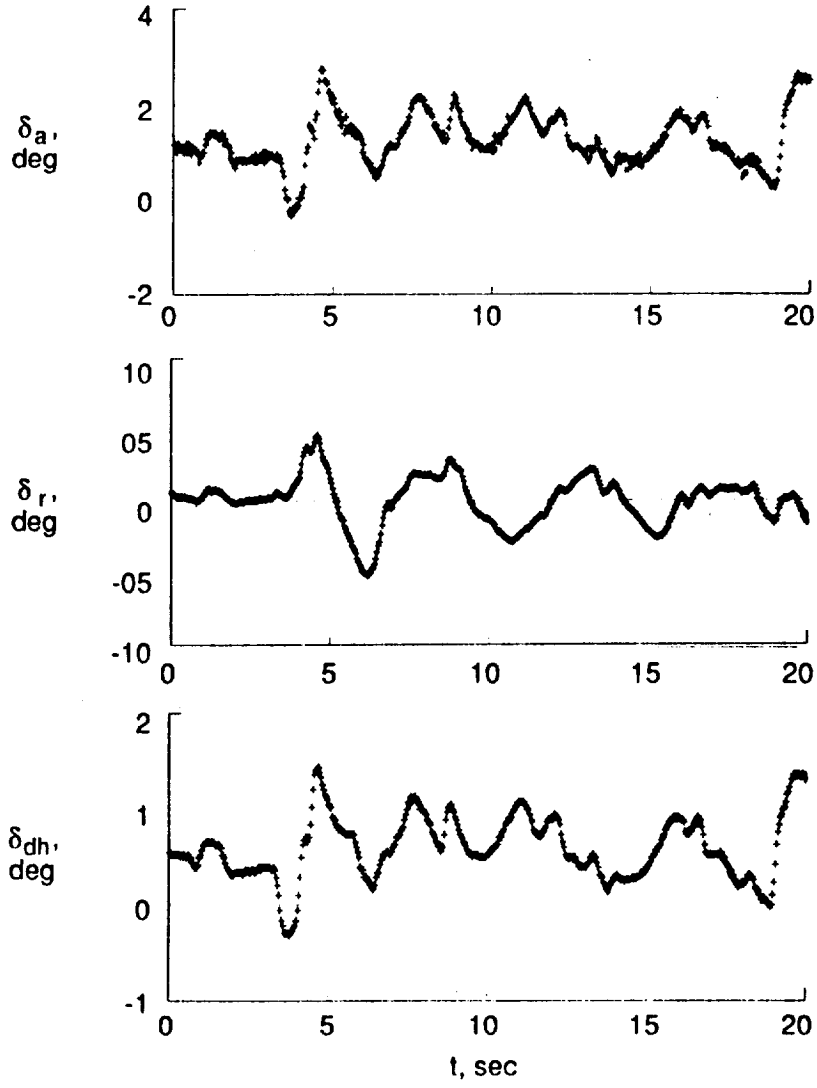

Figure 25. Concluded.

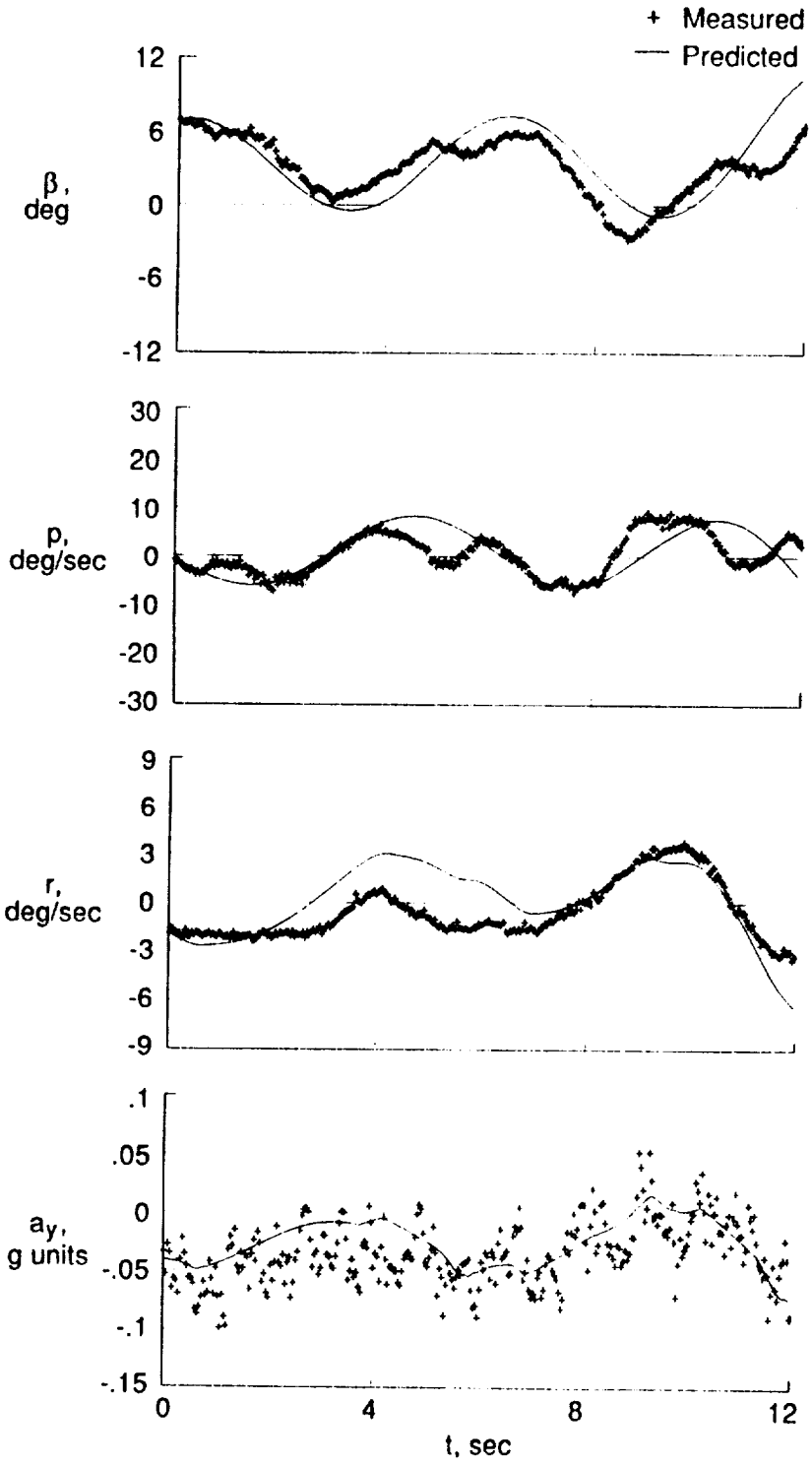

Figure 26 Comparison of measured lateral time histories with those computed. $\alpha_o \approx 48^o$.

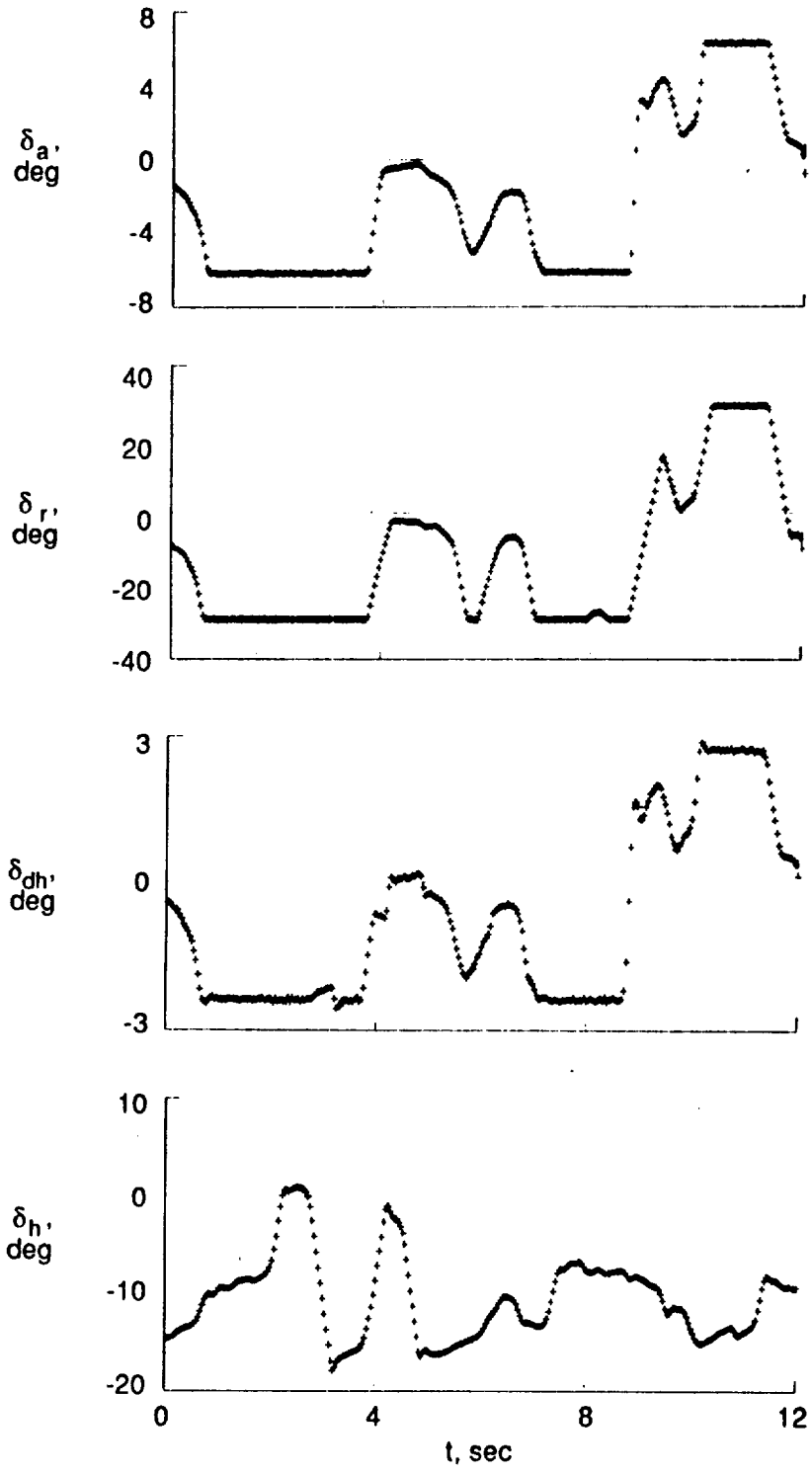

Figure 26. Concluded.

NASA National Aeronautics and Space Administration

Report Documentation Page

1. Report No.	2. Government Accession No.	3. Recipient's Catalog No.
NASA TM-102692		

4. Title and Subtitle

Aerodynamic Parameters of High-Angle-of-Attack Research Vehicle (HARV) Estimated From Flight Data

5. Report Date

August 1990

6. Performing Organization Code

7. Author(s)

Vladislav Klein
Thomas R. Ratvasky
Brent R. Cobleigh

8. Performing Organization Report No.

10. Work Unit No.

505-68-71

9. Performing Organization Name and Address

NASA Langley Research Center
Hampton, VA 23665-5225

11. Contract or Grant No.

13. Type of Report and Period Covered

Technical Memorandum

12. Sponsoring Agency Name and Address

National Aeronautics and Space Administration
Washington, DC 20546-0001

14. Sponsoring Agency Code

15. Supplementary Notes

Vladislav Klein, Thomas P. Ratvasky, and Brent R. Cobleigh, The George Washington University, Joint Institute for Advancement of Flight Sciences, Langley Research Center, Hampton, Virginia

16. Abstract

Aerodynamic parameters of the High-Angle-of-Attack Research Aircraft (HARV) were estimated from flight data at different values of the angle of attack between 10° and 50°. The data were analyzed by a stepwise regression method for obtaining a structure of aerodynamic model equations and least squares parameter estimates. Because of high data collinearity in several maneuvers, some of the longitudinal and all lateral maneuvers were reanalyzed by using two biased estimation techniques, the principal components regression and mixed estimation. The estimated parameters in the form of stability and control derivatives, and aerodynamic coefficients were plotted against the angle of attack and compared with the wind tunnel measurements. The influential parameters are, in general, estimated with acceptable accuracy and most of them are in good agreement with wind tunnel results. The simulated responses of the aircraft showed good agreement with wind tunnel results. The simulated responses of the aircraft showed good prediction capabilities of the resulting model.

17. Key Words (Suggested by Author(s))	18. Distribution Statement
model structure determination parameter estimation linear regression parameter and model verification	Unclassified - Unlimited Subject Category 08

19. Security Classif. (of this report)	20. Security Classif. (of this page)	21. No. of pages	22. Price
Unclassified	Unclassified	68	A04

NASA FORM 1626 OCT 86